Geochemical fingerprinting of Australia's youngest volcanoes: The Newer Volcanic Province, South Australia and Victoria

Thesis submitted in accordance with the requirements of the University of Adelaide for an Honours Degree in Geology/Geophysics

James David George Launder

November 2017

THE UNIVERSITY of ADELAIDE

Geochemical fingerprinting of Australia's youngest volcanoes: The Newer Volcanic Province, South Australia and Victoria

RUNNING TITLE: GEOCHEMICAL DESCRIMINATION OF NVP TEPHRA

ABSTRACT

Traces of volcanic tephra, known as cryptotephra can provide an important isochronous marker that allows sedimentary archives to be aligned in space and time. However, this use of cryptotephra requires an understanding of the unique chemical fingerprint of the glass shards that originate from a particular volcano. Subsequently, this study investigates how the geochemical composition of volcanic centres varies between volcanic centres using collected samples from 9 volcanoes within the NVP, SA and Victoria. Analysis of geochemical data was obtained through laser ablation ICP-MS, to augment previously analysed electron microprobe data for 7 of the 9 sites. This study also investigates the viability of trace element analysis of cryptotephra grains through laser ablation as a useful addition to the major oxide analysis that can be carried out by electron microprobe. Statistical models of linear regression analysis, regression trees and KS-tests, were employed to identify the degree to which the volcanoes studied can be discriminated according to their elemental composition, on the basis of their major oxides and trace elements. The experimental results indicate that a quantifiable difference in major and trace elemental composition can be determined for all volcanic centres analysed except samples obtained from Warrnambool. Subsequently, this study has successfully identified 8 volcanoes with tephra and crypyotephra that

possess specific geochemical fingerprints.

KEYWORDS

Geochemical Fingerprinting, Quaternary, Newer Volcanic Province, Tephra, Major Oxide, Trace Element, LA-ICP-MS

TABLE OF CONTENTS

LIST OF TABLES

LIST OF FIGURES

1. INTRODUCTION

Within recent years, the field of tephrochronology has evolved to become of the most widely used techniques for the correlation of geographically spaced stratigraphical sequences. This process is aided by the distinct geochemical composition of trace and major elements of pyroclastic shards (Hanson, 1980), near instant deposition and wide spatial dispersion of each eruption site (Blockley et al., 2005; Lowe and Alloway, 2015). These properties have resulted in a highly valuable dating tool for sedimentary sequences, used to correlate climactic events and verify previously uncertain dating techniques, which, in the future could potentially lead to a broader understanding of Australian geology as a whole (Lowe, 2011; Smith et al., 2017; Davies, 2015). The study of tephra has seen global success in dating geological and environmental sequences since the 1990's, however, as of yet it remains a mostly untapped resource in Australian geological research (Lowe, 2011).

The tephra deposited from an eruption centre will take one of two forms depending on the magnitude of the eruption and the distance from the eruption centre, the first being a thin layer of pyroclastic rock and tuff close to the volcano. The second, known as cryptotephra, are located at greater distances from the eruption vents, and are more difficult to locate as they consist of microscopic, scattered shards that must be separated from sediment or soil profiles through techniques such as x-ray fluorescence or magnetic susceptibility (Davies, 2015, D'Anjou et al., 2014).

A key method of distinguishing the unique composition of eruption events is the usage of Laser Ablation ICP-MS. Due to high precision of this technique, Laser Ablation ICP-MS is capable of accurately analysing the relative abundance all major oxides and over 30 different trace elements even in shards as small as 40μm (Pearce et al., 2007; Pearce,

2014). This is particularly useful, as trace elements can be used to aid in distinguishing tephra that possess similar concentrations of major oxides (Abbott et al., 2013; Housley et al., 2013). This makes it possible to determine the differences in geochemical composition in even near-identical eruptions through the slight differences in geochemical composition within the ejected tephra. However, to date trace elements have seen little use in the analysis of cryptotephra grains below 15-20 microns due to the background interference, despite recent improvements in detection limits and noise compensation (Pearce, 2012).

A region of particular interest to Australian geological studies is the Newer Volcanic Province within south-eastern Australia, which contains over 400 eruption centres and the youngest volcanic centres within Australia, and is currently a major region for Quaternary paleoclimate research using lake sediments (Gouramanis et al., 2013). Within the NVP, two of the most recent volcanoes, Mt Gambier and Schank (South Australia) have been well studied. They are located approximately 10 km apart within the south-east of South Australian, and both formed within the last 10000 years (e.g. Barbetti and Sheard, 1981; Leaney et al., 1995; Blackburn et al., 1982).

To date, very few studies have explored the occurrence of tephra/cryptotephra in Australian lake sediments, and fewer still have examined the geochemical signatures of tephra from known volcanic sources. To date, two studies have described cryptotephra in lake and wetland sediments: Coulter et al. (2009), using major oxide and trace element data and Smith et al. (2017), using major oxide data. In addition, unpublished major oxide data exists Lake Wangoom (Coulter, 2007). These studies successfully dated the analysed tephra, however only Coulter (2009), using trace element analysis was able to definitively identify the source volcanoes.

Therefore, if these eruptions could be accurately dated and distinguished, they could provide an improved record of Quaternary climate and environmental change. However, at the present more information is needed about the deposition history of the Newer Volcanic Province.

This study will involve testing the both the trace and major elemental composition of tephra and cryptotephra obtained from 9 volcanic centres throughout the region against one another via a combination of previously analysed electron microprobe data (Coulter, 2007), and newly obtained Laser Ablation Inductively Coupled Plasma Mass Spectrometry (LA ICP-MS) of sub-100-micron glass shards, and subsequent statistical analysis in order to determine if the products of the Newer Volcanic Province volcanoes are distinguishable. The study will test the hypothesis that each volcano can be distinguished based on a unique geochemical signature, which can then be used to identify the volcanic source when cryptotephra are discovered in distal sediment deposits. The study will further test the hypothesis that the analysis of trace elements using LA-ICP-MS provides a more discriminating tool than relying solely on major elements, as obtained by electron microprobe. This study provides new insight on the degree of variation across the NVP eruption centres, and will help produce a regional history of the NVP from a geochemical perspective.

Figure 1. Map of South-eastern Australia, highlighting sampling locations and state boundaries. Scale is in 200 km.

Figure 1. Map of South-eastern Australia, highlighting sampling locations and state boundaries. Scale is in 200 km.

2. BACKGROUND

The newer volcanic province of South-Eastern Australia is an intra-plate complex of over 416 monogenetic volcanic centres and 700 eruption points that cover approximately 19, 000 square kilometres throughout Victoria and South Australia (Boyce, 2013). It is believed to have first originated approximately 4.5 million years ago, due to either edge driven convection or mantle plume activity, although currently neither the exact date nor cause is known for certain (Jordan et al., 2012; Demidjuk et al., 2007).

While the Newer Volcanic Province is currently dormant, it remains home to Australia's youngest volcanoes, Mounts Gambier and Schank. These volcanoes erupted approximately 5000-7000 years ago (Barbetti and Sheard, 1981; Leaney et al., 1995; Blackburn et al., 1982, Smith et al., 2017) and, as with all other NVP eruption centres,

formed as short lived, basaltic monogenetic eruptions in the shape of maar and scoria/tuff cone complexes (van Otterloo and Cas, 2013). Other young volcanoes within the region include Mt Eccles and Lake Keilambete, which both erupted ~30,000 years ago as a scoria hill and a maar crater respectively and Tower Hill, at ~ 35000, which erupted as a series of scoria cones (Sherwood et al., 2004).

However, while many monogenetic volcanoes are relatively simple, consisting of small volumes of rapidly rising mantle-derived magma, The Mt Gambier volcanic centre shows remarkable complexity. This is a result of the simultaneous eruptions of two separate magmatic batches, SiO_2 and CaO enriched trachybasalt in the east, and a more alkaline and light REE enriched basanite to the west across over 14 eruption vents. This, in addition to the alternating magmatic and melting-derived phreatomagmatic eruption styles across the vents, has resulted in 20 different stratigraphical units across the complex. These units have been further grouped into six major facies based on their distinctive characteristics (van Otterloo and Cas, 2013).

.

3. METHODS

3.1 SAMPLE COLLECTION AND PREPARATION

Samples from proximal tephra deposits from Mt Eccles, Mt Noorat, Mt Warrnambool, Lake Terang, Lake Wangoom, Lake Keilambete and Tower Hill volcanoes within Victoria by Dr Sarah Coulter (formerly of Queen's university, Belfast) These samples consisted of volcanic glass shards mounted on glass slides, having previously been analysed through an electron microprobe. Additional samples were collected from Mt Gambier and Schank, South Australia at seven outcrops (Figure 2) identified by previous geological and environmental studies (Lowe, 1992; van Otterloo and Cass,

2013; Smith and Prescott, 1987; van Otterloo et al., 2013), with two collected from Mt Schank, and five at Mt Gambier. A geological hammer was used in order to remove the weathered surface and obtain fresh material, which was subsequently placed within a sealed plastic container for transport.

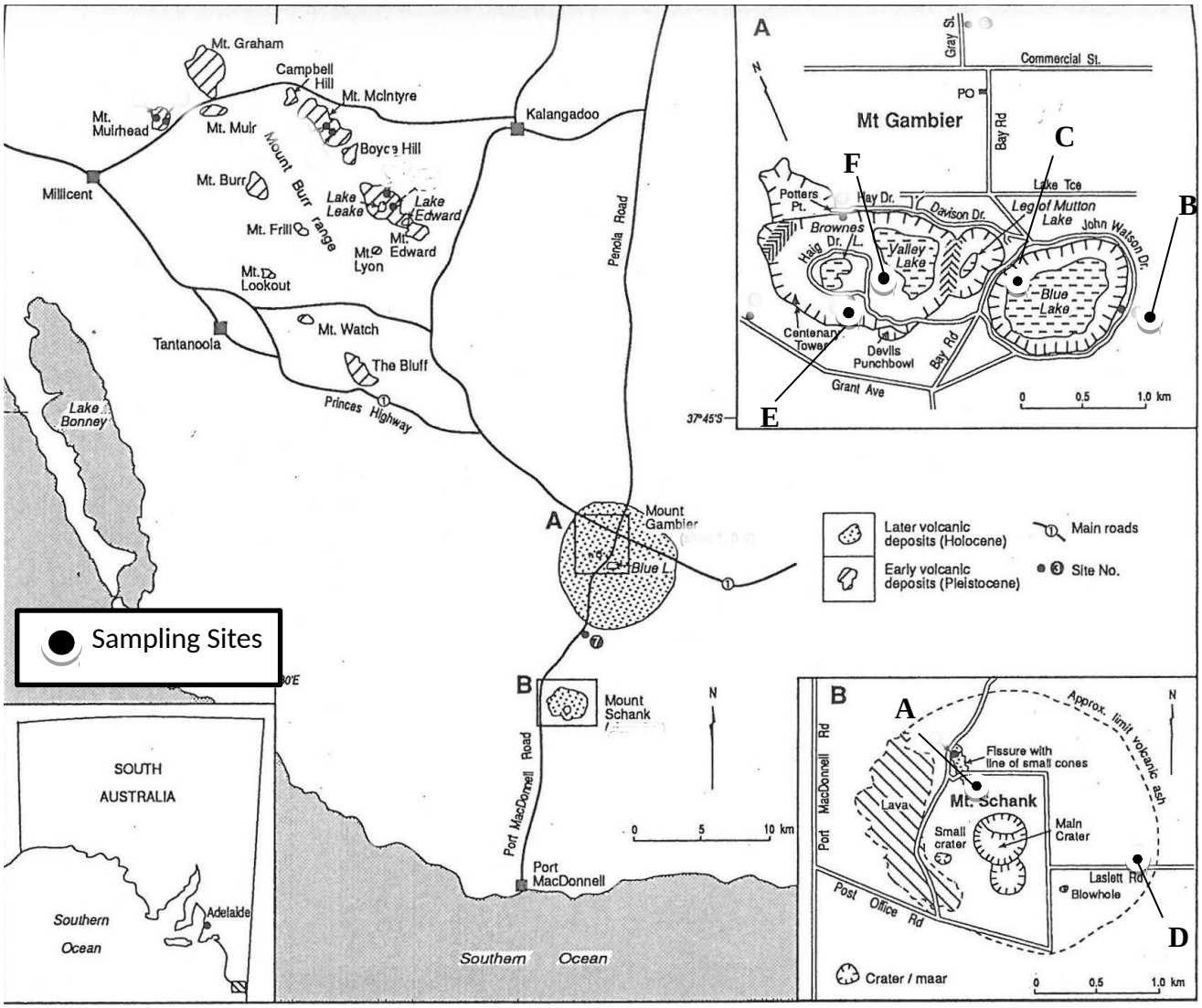

Figure 2. Location Map of Mt Gambier and Mt Schank in South Australia. 1a location map of sampling sites B, C, E, F within Mt Gambier volcanic centre, 1b location of Mt Schank sampling sites A, D, highlighted as black circles. (adapted from Lowe CSIRO Report, 1992).

Each of the samples obtained from Mt Gambier and Mt Schank were washed using 10% HCl solution for 30 min at room temperature, before rinsing twice with deionised water, and sieved using a 250, 125 and 40-micron sieve to separate sediments for analysis and

remove clays and organics. The samples were warmed in a 40ºC oven for 2 hours to evaporate the remaining water, and analysed under a binocular microscope at 20x magnification to identify and isolate the volcanic glass from each sample.

Scoria clasts were identified in all size fractions, but particularly in the >250 microns fractions. These clasts were isolated and crushed using a mortar and pestle, and the resulting volcanic glass was, sieved using a 40-micron sieve to remove small particles and dried overnight in a 40ºC oven. Samples from each location were embedded in epoxy resin and polished.

3.2 GEOCHEMICAL ANALYSIS OF MAJOR OXIDES AND TRACE ELEMENTS

The prepared NVP tephra and cryptotephra samples were analysed through Laser Ablation ICP-MS using a RESOlution ArF excimer 193nm laser (Australian Scientific Instruments) coupled to an Agilent 7900x ICP-MS. Samples from Mt's Gambier and Schank were analysed using a spot size of 29 µm, pulse rate of 5Hz, attenuation of 100%, energy of 30mJ and a fluence of 3.5 J/cm2 with He as the ablation gas. Cryptotephra samples from Victoria were analysed using a spot size of 13-19 µm, pulse rate of 5Hz, attenuation of 30%T, energy of 105mJ and a fluence of 3.5 J/cm2. For each analysis 30 seconds of background was collected with the laser switched off, followed 30 seconds of ablation. Basaltic glass GSD-1G was used as the external standard, and ^{27}Al as the internal standard element for quantification for Gambier and Schank, and the sodic glass NIST612 and ^{27}Al were used as the external and internal standards for the Victorian cryptotephra samples. Beam intensities of ^{27}Al, ^{23}Na, ^{24}Mg, ^{28}Si, ^{31}P, ^{39}K, ^{40}Ca, ^{48}Ti, ^{51}V, ^{52}Cr, ^{55}Mn ^{56}Fe, ^{88}Sr, ^{91}Zr, ^{137}Ba, ^{45}Sc, ^{85}Rb, ^{89}Y, ^{93}Nb, ^{133}Cs, ^{139}La, ^{140}Ce, ^{141}Pr, ^{144}Nd, ^{150}Sm, ^{152}Eu, ^{157}Gd, ^{159}Tb, ^{163}Dy, ^{165}Ho, ^{167}Er, ^{169}Tm, ^{173}Yb, ^{175}Lu, ^{178}Hf, ^{181}Ta, ^{207}Pb, ^{232}Th, ^{238}U were measured.

This data was processed though Iolite software (Hellstrom et al., 2008) in order to remove ablations that failed to detect sufficient tephra for analysis and isolate and remove the background to generate a stable signal. The concentration of the Major and Trace elements of each sample was obtained in parts per million by normalising data to 100% using the internal standard ^{27}Al. The data was processed in excel to remove elements below the detection limit of the laser.

3.3 STATISTICAL ANALYSIS

The differences in composition of trace elements and major oxides was processed using the R software package (R Core Team, 2013) to generate box and whisker plot diagrams to provide information on the distribution of elements on single elements between volcanoes based upon their interquartile range, which accounts for 1.35 standard deviations from the mean and whiskers, which account for all data barring discarded outliers. and Kolmogorov-Smirnov analysis on pairs on pairs of samples and elements to test the null hypothesis that there is no significant difference between the concentration of elements if the p-value > 0.05. In addition, linear discriminant analysis was performed through the Vegan and MASS software packages (Venables and Ripley, 2002; Oksane et al., 2017, Curran, 2017) to test how the collective suite of elements can discriminate using a linear combination of features that characterise or separate the volcanic centres, elements containing high lambda values relative to the other elements analysed are better discriminants. A final analysis through the usage of regression trees utilising the rpart software package (Therneau et al., 2017) provided a reference tool for tracking the provenance of a glass shard based on their elemental composition as % total mass.

4. RESULTS

4.1 DETECTION LIMIT AND UNCERTAINTY ANALYSIS

Elements with concentrations below detection limit were excluded from subsequent analysis. The particle size of samples from Mt's Gambier and Schank were in the range 250-40 microns, from 13 samples from Mt's Gambier and Schank were determined to contain one or more elements below detection limits via LA ICP-MS, and were excluded from analysis. By contrast, samples from the other 7 sites were in the range of 100-15 microns, such that 126 samples were excluded.

The analysis of the uncertainty associated with element between volcanos shows average uncertainty values below 20% for most elements analysed at 7 of the 9 sites, with an average uncertainty of ~10% for the analysed major oxides and ~20% for trace elements. However, an average uncertainty of above 30 % was determined for the least abundant trace elements, Tb, Ho, Er, Tm, Yb and Th across 6 of the 9 volcanic samples, which were excluded from further analysis, and consistent significant uncertainty above 30% across samples from Mt Eccles and Lake Warrnambool (Table 1).

Table 1. Mean concentration and associated % uncertainty of each analysed element as % total mass within each location.

	SCH	GAM	ECCL	KEI	NOOR	TERA	TOWE	WANG	WARR
Al_2O_3	15.64281±4.6%	14.8097±5.3%	19.90513±7.3%	21.82098±4.8%	18.45757±2.9%	26.27675±10.7%	17.94748±1.9%	14.75873±4.2%	25.07416±6.6%
Na_2O	5.28872±1.7%	4.80444±1.9%	3.27693±8.1%	1.49190±9.3%	4.06562±3.2%	3.11763±8.9%	3.65925±2.0%	2.52009±4.3%	1.98198±7.2%
MgO	3.90192±2.1%	5.18525±2.6%	3.69197±3.6%	2.31489±5.0%	3.60738±4.5%	2.39386±17.5%	3.99138±1.6%	9.24718±5.9%	1.75620±7.8%
SiO_2	50.446733±1.0%	49.06530±1.2%	49.42273±1.8%	50.105144±3.1%	47.851555±1.4%	51.586666±10.8%	49.206988±1.3%	48.475900±1.7%	48.550166±6.0%
P_2O_5	1.17382±1.2%	1.06085±1.5%	0.27058±14.2%	0.77334±11.0%	0.82033±2.1%	0.30772±24.5%	0.81191±1.5%	0.19378±13.9%	0.39489±11.9%
K_2O	3.57089±2.5	3.08510±2.0	1.08316±9.6	2.16908±6.8	2.93620±3.7	1.33697±3.9	2.41220±2.5	0.63558±13.3	2.57204±5.6

	%	%	%	%	%	%	%	%	%
CaO	7.77189 ±2.5 %	8.51868 ±2.3 %	9.83333 ±8.2 %	10.2941 1±13.5 %	9.04369 ±4.7 %	4.49607 ±21.6 %	8.79805 ±3.9 %	15.4677 8±4.9 %	14.1007 9±10.5 %
TiO_2	2.69185 ±1.0 %	2.88745 ±1.3 %	1.83127 ±6.2 %	1.67021 ±7.1 %	2.69952 ±3.1 %	1.70814 ±15.4 %	2.57900 ±2.3 %	1.49044 ±6.1 %	1.31667 ±14.0 %
VO	0.02912 ±1.7 %	0.03528 ±1.9 %	0.02720 ±10.1 %	0.02979 ±5.9 %	0.02678 ±5.5 %	0.02293 ±17.5 %	0.03173 ±2.2 %	0.04049 ±6.6 %	0.02402 ±11.1
Cr_2O_3	0.00585 ±20.6	0.01424 ±9.7 %	0.00987 ±12.2%	0.00813 ±14.7 %	0.00635 ±12.3 %	0.00773 ±16.7 %	0.01087 ±4.8%	0.19336 ±17.0 %	0.00972 ±21.6 %
MnO	0.17427 ±1.3 %	0.18934 ±1.6 %	0.12662 ±11.3%	0.06553 ±7.9%	0.15514 ±4.0%	0.07890 ±12.2%	0.17142 ±2.6%	0.11668 ±6.1%	0.05868 ±15.8 %
FeO	9.01943 ±1.7 %	10.0909 0±2.0 %	10.3750 7±6.8%	9.05309 ±6.2%	10.0830 5±4.0%	8.54673 ±13.9%	10.1615 2±2.6%	6.84292 ±6.4%	5.96907 ±9.9 %
SrO	0.13761 ±1.0 %	0.12233 ±1.3 %	0.06970 ±4.0%	0.11627 ±12.2%	0.12878 ±4.0%	0.05241 ±20.9%	0.11385 ±2.8%	0.08642 ±7.2%	0.11886 ±13.9 %
ZrO_2	0.04866 ±1.3 %	0.04432 ±1.3 %	0.02208 ±18.6%	0.03943 ±9.4%	0.05628 ±3.7%	0.02669 ±21.6%	0.04239 ±2.1%	0.01516 ±8.1%	0.02888 ±17.0 %
BaO	0.09861 ±1.4 %	0.08680 ±2.5 %	0.03318 ±13.9%	0.04872 ±13.9%	0.06174 ±4.1%	0.04081 ±25.8%	0.06197 ±2.8%	0.02739 ±21.8%	0.05952 ±6.7 %
Sc	0.00125 ±8.2 %	0.00163 ±6.4 %	0.00218 ±18.7%	0.00144 ±22.4%	0.00155 ±12.6%	0.00170 ±30.1%	0.00171 ±8.9%	0.00408 ±21.1%	0.00131 ±34.2 %
Rb	0.00756 ±2.1 %	0.00645 ±9.3 %	0.00269 ±21.8%	0.00938 ±10.8%	0.00596 ±6.2%	0.00554 ±25.2%	0.00491 ±5.1%	0.00175 ±28.2%	0.00684 ±20.5 %
Y	0.00266 ±2.6 %	0.00271 ±2.9 %	0.00170 ±20.1%	0.00221 ±20.7%	0.00246 ±6.6%	0.00162 ±30.0%	0.00246 ±4.5%	0.00149 ±14.3%	0.00121 ±28.2 %
Nb	0.00992 ±1.6 %	0.00843 ±2.4 %	0.00344 ±28.2%	0.00606 ±12.5%	0.00860 ±4.2%	0.00380 ±26.5%	0.00673 ±3.2%	0.00143 ±20.7%	0.00463 ±43.3 %
Cs	0.00011 ±12.7 %	0.00009 ±22.3 %	0.00015 ±40.7%	0.00048 ±21.5%	0.00017 ±13.0%	0.00036 ±21.4%	0.00008 ±18.1%	0.00019 ±27.0%	0.00034 ±40.9 %
La	0.00664 ±1.5 %	0.00586 ±2.0 %	0.00231 ±26.6%	0.00452 ±18.6%	0.00552 ±4.8%	0.00198 ±9.7%	0.00463 ±5.8%	0.00135 ±11.1%	0.00220 ±30.4 %
Ce	0.01275 ±1.3 %	0.01135 ±1.7 %	0.00443 ±35.8%	0.00924 ±16.4%	0.01145 ±4.8%	0.00326 ±18.7%	0.00931 ±4.5%	0.00292 ±10.1%	0.00686 ±20.2 %

Pr	0.00140 ±2.4 %	0.00126 ±2.9 %	0.00054 ±30.5%	0.00102 ±21.0%	0.00133 ±7.3%	0.00045 ±8.6%	0.00107 ±6.8%	0.00039 ±14.7%	0.00061 ±33.1 %
Nd	0.00561 ±3.0 %	0.00509 ±3.4 %	0.00261 ±32.8%	0.00416 ±26.1%	0.00543 ±6.4%	0.00240 ±16.3%	0.00454 ±8.4%	0.00184 ±15.9%	0.00253 ±26.7 %
Sm	0.00108 ±6.2 %	0.00102 ±7.3 %	0.00056 ±41.6%	0.00083 ±38.0%	0.00112 ±11.0%	0.00040 ±32.3%	0.00097 ±15.6%	0.00050 ±24.7%	0.00061 ±52.8 %
Eu	0.00034 ±5.9 %	0.00032 ±6.8 %	0.00016 ±30.9%	0.00026 ±37.1%	0.00034 ±11.7%	0.00022 ±31.6%	0.00031 ±11.7%	0.00017 ±19.1%	0.00015 ±42.2 %
Gd	0.00088 ±8.0 %	0.00084 ±8.1 %	0.00056 ±53.5%	0.00062 ±37.0%	0.00089 ±15.4%	0.00089 ±22.4%	0.00083 ±15.5%	0.00053 ±19.0%	0.00038 ±48.4 %
Tb	0.00011 ±7.2 %	0.00011 ±8.1 %	0.00007 ±39.2%	0.00008 ±38.7%	0.00011 ±14.2%	0.00008 ±42.3%	0.00010 ±13.9%	0.00007 ±25.3%	0.00005 ±50.6 %
Dy	0.00062 ±7.4 %	0.00061 ±7.2 %	0.00036 ±38.1%	0.00049 ±40.0%	0.00059 ±11.8%	0.00068 ±40.1%	0.00057 ±12.7%	0.00039 ±20.1%	0.00046 ±21.8 %
Ho	0.00010 ±7.5 %	0.00010 ±8.0 %	0.00007 ±44.8%	0.00008 ±45.9%	0.00010 ±12.4%	0.00006 ±64.4%	0.00009 ±17.0%	0.00006 ±34.0%	0.00004 ±71.5 %
Er	0.00025 ±9.0 %	0.00025 ±9.2 %	0.00017 ±33.5%	0.00020 ±45.5%	0.00023 ±18.7%	0.00015 ±64.0%	0.00023 ±16.4%	0.00017 ±20.4%	0.00010 ±60.1 %
Tm	0.00003 ±13.7 %	0.00003 ±14.4 %	0.00002 ±60.2%	0.00003 ±51.2%	0.00002 ±21.1%	0.00003 ±31.0%	0.00002 ±19.5%	0.00002 ±26.5%	0.00002 ±36.4 %
Yb	0.00018 ±12.7 %	0.00018 ±12.9 %	0.00015 ±50.1%	0.00018 ±47.8%	0.00015 ±18.7%	0.00014 ±14.7%	0.00016 ±18.0%	0.00012 ±24.2%	0.00016 ±28.7 %
Lu	0.00002 ±15.2 %	0.00002 ±16.5 %	0.00002 ±45.9%	0.00003 ±54.2%	0.00002 ±24.8%	0.00003 ±41.5%	0.00002 ±30.8%	0.00001 ±36.2%	0.00001 ±63.9 %
Hf	0.00077 ±5.3 %	0.00071 ±6.0 %	0.00038 ±38.2%	0.00057 ±27.3%	0.00094 ±9.4%	0.00059 ±15.4%	0.00068 ±14.9%	0.00036 ±19.4%	0.00032 ±52.3 %
Ta	0.00052 ±3.6 %	0.00044 ±4.5 %	0.00014 ±31.9%	0.00032 ±23.2%	0.00049 ±9.2%	0.00023 ±30.8%	0.00040 ±11.3%	0.00010 ±28.2%	0.00021 ±41.6 %
Pb	0.00067 ±6.8 %	0.00059 ±7.3 %	0.00074 ±38.1%	0.00140 ±27.6%	0.00087 ±9.3%	0.00156 ±27.7%	0.00053 ±15.1%	0.00020 ±45.2%	0.00107 ±36.1 %
Th	0.00090 ±4.0 %	0.00076 ±4.9 %	0.00040 ±37.2%	0.00085 ±27.3%	0.00074 ±8.7%	0.00047 ±20.9%	0.00057 ±11.6%	0.00015 ±41.9 %	0.00038 ±45.9 %
U	0.00024	0.00020	0.00009	0.00025	0.00019	0.00010	0.00013	0.00005	0.00010

	±6.9 %	±8.6%	±80.3%	±31.8%	±14.2%	±46.2%	±13.2%	±43.1 %	±71.8 %

4.2 COMPARISON OF VOLCANIC CHEMISTRY BASED ON INDIVIDUAL MAJOR AND TRACE ELEMENTS

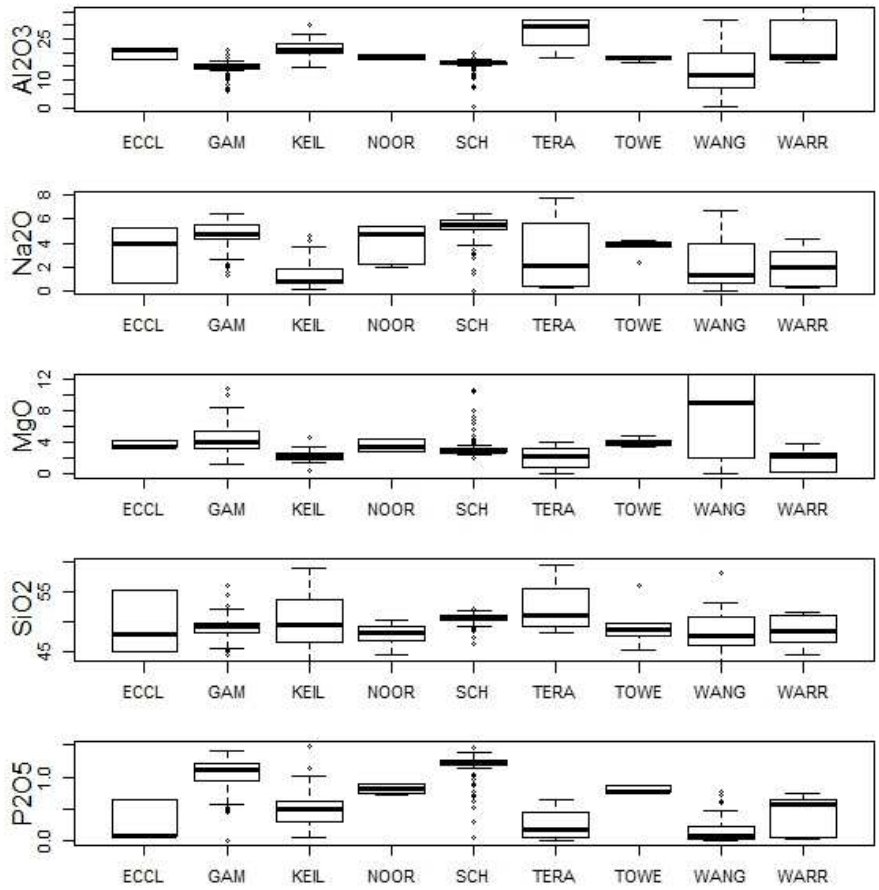

Figure 3. Box and whisker plot of Al_2O_3, Na_2O, MgO, SiO_2 and P_2O_5, as analysed by LA ICP-MS. Values are obtained from all samples as a % concentration of total.

Box and Whisker plots of each element used in the analysis were generated using major oxides, trace element and electron microprobe data. Box plots derived from electron microprobe data show small interquartile ranges which rarely exceeded a ± 15% from the median concentration value among all sites and major oxides, and rare overlap

between sites. Keilambete possesses high K_2O and Al_2O_3 relative to other sites, while Eccles possesses high concentrations of CaO and low Al_2O_3, and Wangoom higher TiO_2 than any other sampling location. Furthermore, Noorat and Terang possess unique FeO concentrations, and Tower Hill possesses intermediate SiO_2 while all other sites possess high, or low concentrations. Warrnambool contains the low concentrations of SiO_2.

Box plots taken from Major oxide La ICP-MS data suggests that the concentration of major oxides within the volcanic centres possess small interquartile ranges of ~ ± 15% of median for 5 of the 9 sites. Mt Schank possesses high concentrations of P_2O_5, K_2O and BaO, while Mt Gambier contains high TiO_2 and MnO, Tower hill contains intermediate TiO_2 while Noorat has high ZrO_2. However, Eccles, Terang, Wangoom and Warrnambool possessed large interquartile ranges at or above ± 50% for most elements barring those of high concentration such as SiO_2 or Al_2O_3, making separation between each other and the other sites difficult (Figure 3).

Box plots generated from trace element data shows some variation in concentration between volcanic centres, however most sites possess interquartile ranges that exceeded ± 50% of the median throughout each element, and large overlap. Mt Gambier, Mt Schank and Tower hill data appears to be the only locations with interquartile ranges consistently below ± 20%. Some unique compositions exist, such as Y in the case of Mt Gambier, and Nb in Mt Schank, low Cs in Wangoom, however, all other elements show overlap for all sites with a minimum of one other site.

The p-values calculated by KS-tests of all trace and major elements analysed for Mt Gambier and Mt Schank shows a statistical difference between the majority of the element concentrations of the two volcanoes. All elements except Dy and Tm possess a p-value below 0.05, rejecting the null hypothesis that there is no difference between the means of the elements, and that a significant difference exists.

4.3 LINEAR DISCRIMINANT ANALYSIS

LDA was performed for major oxides analysed by electron microprobe for all sites, except Mt's Gambier and Schank, for which LA ICP-MS data was used, and then for trace element data in which case all elemental data was generated by LA ICP-MS. The electron microprobe data showed a significant degree of clustering amongst samples from the same site, and large spacing between locations with only Warrnambool indistinguishable from other locations, and high lambda values relative to other oxides for MgO, Al_2O_3 and CaO, which indicates that these major oxides are a useful discriminant for all sites except Warrnambool (Figure 4).

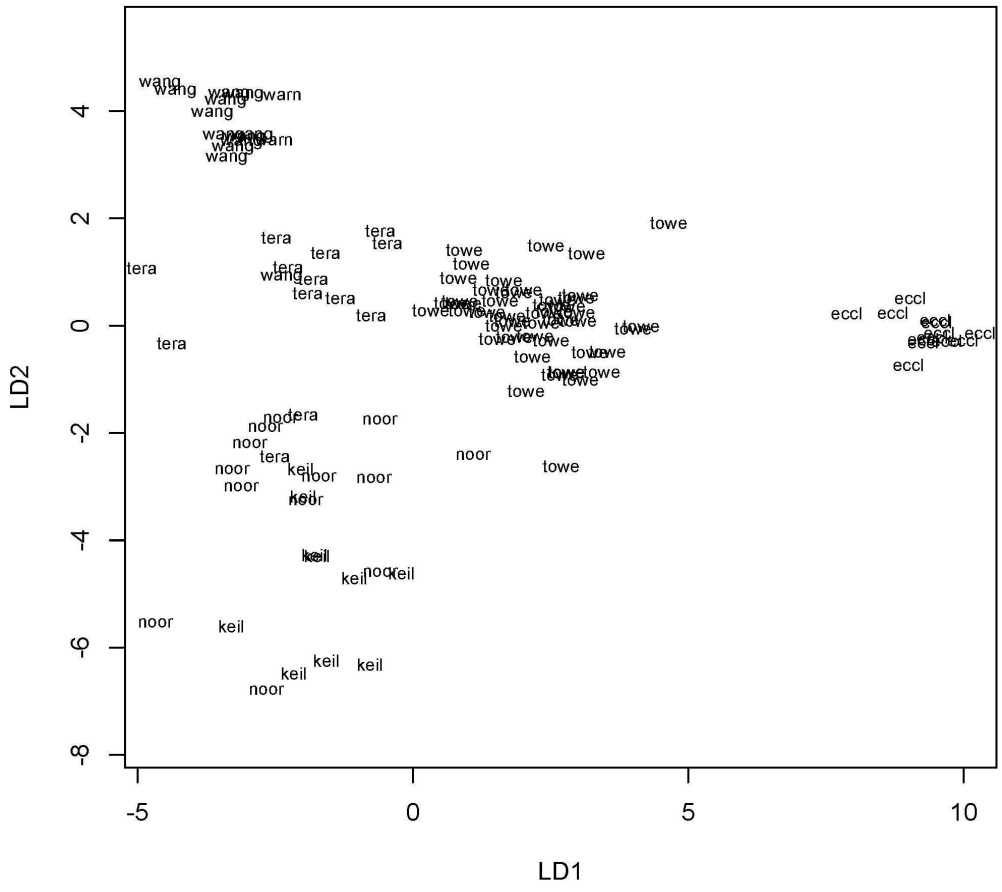

Figure 4. Linear Discriminant Analysis model of NVP eruption centres derived from electron microprobe data.

LD1 represents discriminants capable of separating sites on the x-axis, LD2 represents discrimination on y-axis. Large spacing between sites suggests large differences in composition, multiple sites in same region of space suggests no difference exists between samples

When analysing LDA with LA ICP-MS data, analysis including samples from Mt Gambier and Mt Schank showed that the clustering of Victorian samples could not be accurately analysed due to the large difference in sample size between the two data sets (Figure 5a), however high lambda values were found for VO and ZrO_2. The analysis was repeated without the presence of Mt Gambier or Schank data, and subsequent plots showed improved clustering of samples (Figure 5b), and the same elements possessing high lambda. The resulting major oxide ablation data contained significant scatter among samples, with no visible grouping present for samples from Warrnambool, Noorat or Terang.

LDA of trace element data also possessed significant degree of scatter between samples of the same site, with only Wangoom, Keilambete, Tower Hill and Terang samples showing any degree of grouping. High lambda values were found for Cs, Pr, Eu, Ta and Pb.

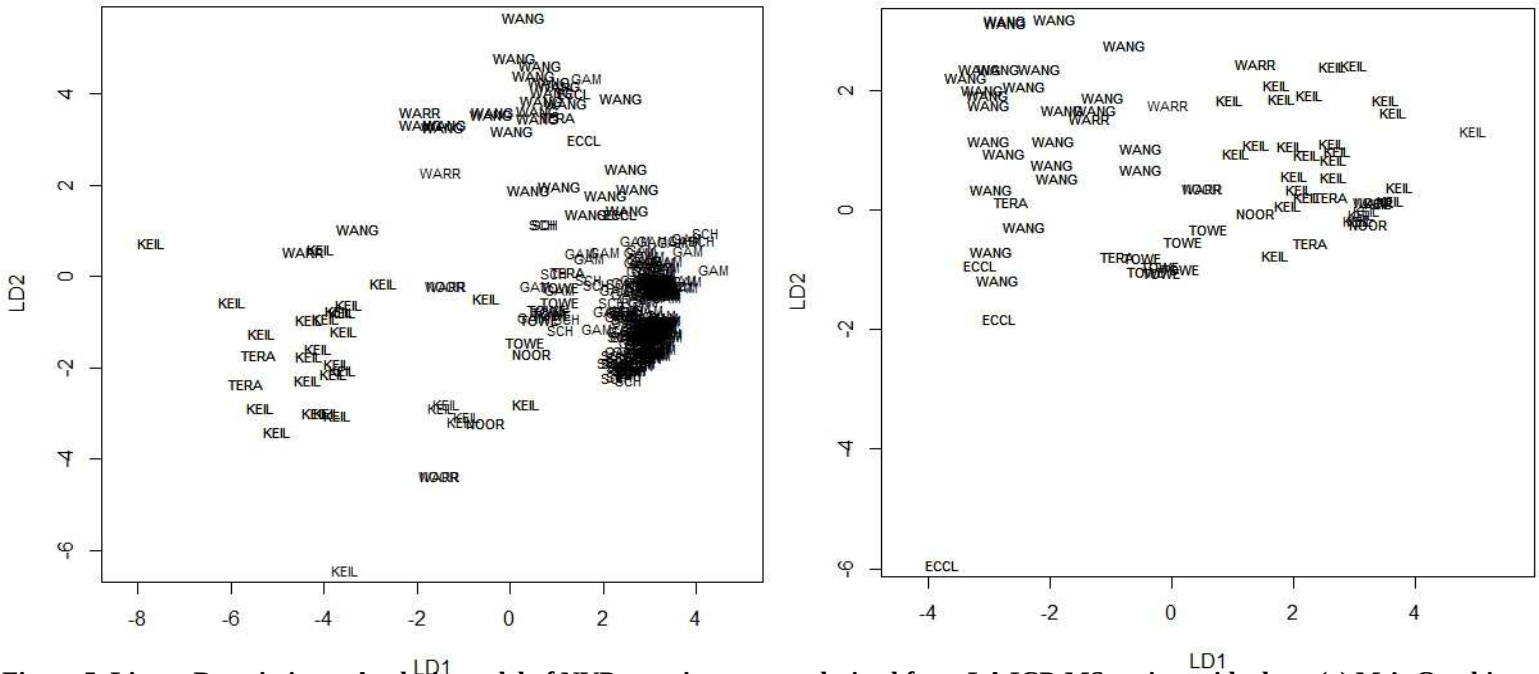

Figure 5. Linear Descriminant Analysis model of NVP eruption centres derived from LA ICP-MS major oxide data, (a) Mt's Gambier and Schank included, and (b) Mt Gambier and Schank excluded. LD1 represents discriminants capable of separating sites on the x-axis, LD2 represents discrimination on y-axis. Large spacing between sites suggests large differences in composition, multiple sites in same region of space suggests no difference exists between samples

4.4 REGRESSION TREE ANALYSIS

Individual regression tree plots were created for major oxide, trace element and electron microprobe analysis of NVP volcanics, with Mt Gambier and Schank data included in all instances. The electron microprobe data was capable of distinguishing all sites except Warrnambool based upon individual major oxides. For example, Terang can be separated based upon MnO ≥ 0.18% and MnO > 0.2331%, or MnO ≤ 0.18%, SiO_2 ≤ 48.91%, Na_2O > 4.146%, Na_2O ≥ 4.868% and SiO_2 ≤ 48.28%, while Tower Hill can be distinguished through MnO ≥ 0.18%, MnO < 0.2331%, CaO > 9.244% and Al_2O_3 > 14.52%.

Regression trees of the Major oxide LA ICP-MS data isolated 7 of the 9 analysed sites, such as Tower Hill, through MnO ≥ 0.18%, Na_2O ≤ 4.09% and MgO ≤ 4.89, however, it was unable to distinguish Noorat and Warrnambool (Figure 6),

The Trace element data separated 7 of the 9 sites Based upon slight variations in trace elements, such as Terang based upon Pb ≥ 0.00085%, U ≤ 0.00018% and Eu > 0.00011%, or Noorat though Pb ≤ 0.00085%, Rb < 0.0077%, Rb ≥ 0.004, Tm ≤ 2.6×10^{-5}, Eu > 0.0003 and Ce ≥ 0.011, but was incapable of distinguishing Eccles and Warrnambool though any trace elements.

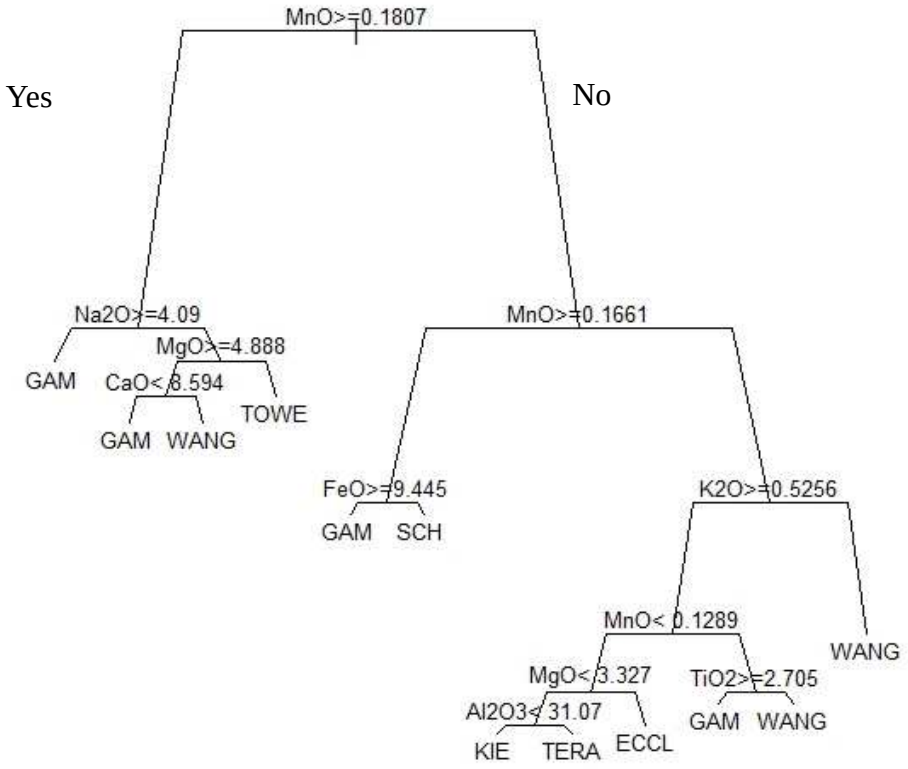

Figure 6. Regression tree of LA ICP-MS major oxide data at all sites. Sites not present within tree are not distinguishable based upon major oxides. Sites are distinguished based on the combination of oxide concentrations in % total concentration. If the value is true

5. DISCUSSION

The ability to geochemically fingerprint volcanic tephra and cryptotephra is central to their value as isochronous markers in sedimentary sequence. This study examined the major and trace element composition of glass shards from 9 sites within the NVP, Victoria and South Australia, demonstrating that unique geochemical signatures can be assigned to the sites studied.

5.1 The use of major elements to discriminate volcanic glass provenance

Previous studies into the geochemical composition of glass shards from late Quaternary volcanoes within the NVP are rare. Coulter (2007) examined 7 sites using electron microprobe analysis and ternary diagrams, and the study concluded that only Mt Eccles

could be adequately distinguished from all other sites through its FeO content. The results of this study indicate that these volcanoes can indeed be discriminated, largely due to the application of alternative strategies for displaying and analysing the data. Box plots constructed from the oxide data possess small interquartile ranges that rarely surpass ± 15% of the median value, and decreases significantly within elements of higher concentrations, with few instances of overlap between the interquartile ranges of sites and few outliers within each element. Subsequently, these results suggest that all sites can be successfully distinguished from one another with a minimum of 50% chance of accuracy, and Keilambete and Eccles can be separated based on their K_2O, and CaO and MgO with 100% accuracy respectively, as noted by lack of overlap between whiskers. This suggests that the volcanoes within the Newer Volcanic Province can be accurately discriminated based upon their major oxides.

A Linear discrimination analysis of the electron microprobe data shows significant grouping of samples within each site, and large special separation between sites through the x and y-axis, signifying large variations in composition between sites (Figure 4). However, Warrnambool was not distinguishable from other sites using this method. The major oxides determined to be of significant use to the discrimination of all sites except Warrnambool were MgO, Al_2O_3 and CaO, which agrees with the major discriminants determined within the box and whisker plots. Subsequent analysis through a regression tree further supported this assessment, separating all but Warrnambool through the variations in the concentrations of MnO, Al_2O_3, SiO_2, Na_2O, TiO_2 and CaO. For example, Terang was distinguishable within the regression tree concentrations of MnO ≥ 0.18% and MnO > 0.23%. These major oxides also agree with the results of the box plot diagrams for all elements except MnO, which does not appear to discriminate within the box plots. This suggests that simple tests such as box plot diagrams may not

be sufficient when attempting to separate major oxides and elements which possess larger interquartile ranges, like those seen for MnO.

While these analyses were unable to geochemically fingerprint Lake Warrnambool, only 2 samples from Warrnambool were used in the electron microprobe analysis, while every other site used within the analysis used a minimum of 10, which occurred because the samples taken from the site were very small and contained a high concentration of inclusions (Coulter, 2007). Therefore, it is likely that the lack of a geochemical fingerprint for Warrnambool is due to error, rather than possessing highly variable concentration across its eruption centre.

In addition, new data from Mt Gambier and Schank was in conjunction with the LA ICP-MS data of the Victoria cryptotephra in order to attempt to separate the volcanic centres using LA ICP-MS. Box plots were constructed for each major oxide to compare the relative concentrations of each site. Mt Schank, Mt Gambier and Noorat can be distinguished from every other site within the analysis based upon; P_2O_5, K_2O and BaO in the case of Schank, TiO_2 and MnO for Gambier and ZrO_2 for Noorat. However, each other site overlaps to some degree with at least one other, so it may be necessary to use the full range of compositions to separate the volcanic centres rather than singular oxides. For example, Tower Hill can be separated from Keilambete, Terang, Wangoom and Warrnambool based upon its high MnO values, and the remaining volcanoes (Figure 3), Schank, Noorat and Gambier based upon its intermediate K_2O. It is also possible that the large interquartile ranges observed within these plots are the result of error within the samples, as the sites that show the largest ranges of composition coincide with the volcanic centres possessing the largest uncertainty values, which is further supported by the small interquartile ranges observed within the electron microprobe data for the same sites.

A linear discriminant analysis conducted on the sites being tested showed little variation between sites while sample data from Mt's Gambier and Schank was present, which was likely due difference in sample size between their samples and those derived from the Victorian cryptotephra, resulting in a smaller confidence in separation in the sites containing fewer samples. Subsequently, a second test was run without Gambier or Schank which showed some improvement to the data with 4 of the 7 volcanic centres showing grouping, however the attempt to distinguish all of the volcanic centres based on a linear discriminant analysis was a failure. Furthermore, the discriminatory elements determined by the LDA, VO and ZrO_2, do not agree with those found for the electron microprobe data. This was determined to be a result of the small sample size present for Mt Eccles, Noorat and Warrnambool, which often causes instability in the analysis due to a lack of information (Tebbens and Schlesinger, 2007).

Table 2. Number of samples used in statistical analysis of each site using LA ICP-MS and Electron Microprobe.

	LA ICP-MS	Electron Microprobe
Mt Gambier	175	-
Mt Schank	108	-
Mt Eccles	6	13
Lake Kielambete	53	10
Mt Noorat	6	13
Lake Terang	8	14
Tower Hill	14	50
Lake Wangoom	52	13
Mt Warrnambool	7	2

A regression tree analysis was run to better discriminate the volcanic centres based on individual major oxides, and was able to discriminate all volcanic centre except Noorat and Warrnambool, and in the case of Mt's Gambier and Wangoom, was capable of discriminating based upon multiple major oxides. For example, Mt Gambier could be discriminated using multiple combinations of concentrations such as MnO $\geq$ 0.18%

and $Na_2O \geq 4.09\%$, or $MnO \geq 0.18\%$, $Na_2O \leq 4.09\%$, $MgO \geq 4.89\%$ and $CaO < 8.59\%$ etc., while Schank could only be discriminated through $MnO \leq 0.18\%$, $MnO \geq 0.166\%$ and $FeO \leq 9.45\%$ (Figure 6). However, while these agree with the electron microprobe LDA discriminatory oxides they do not agree with those determined during LA ICP-MS LDA, which suggests that an error may have occurred during the LDA analysis of the data.

An uncertainty analysis performed upon the LA ICP-MS data shows that the tephra obtained from Gambier and Schank possessed an uncertainty value below 5% for all major oxides except Cr_2O_3, which was further supported by a comparison of average concentration against prior tests of Mt Gambier and Schank SiO_2 (48-50 wt. %), and Al_2O_3 (~16 wt. %) (Lowe et al., 1996; Lowe and Palmer, 2005). However, the Victorian cryptotephra samples showed significantly greater uncertainty throughout the major oxides, averaging close to 10%. Eccles, Terang and Warrnambool in particular showed significant uncertainty above 15% in all but the most abundant oxides such as SiO_2. This is likely to have occurred because of the small beam size required to analyse these samples, as ions formed by the plasma create a large amount of background noise, which results in decreased precision below 20 microns (Petrelli et al., 2016).

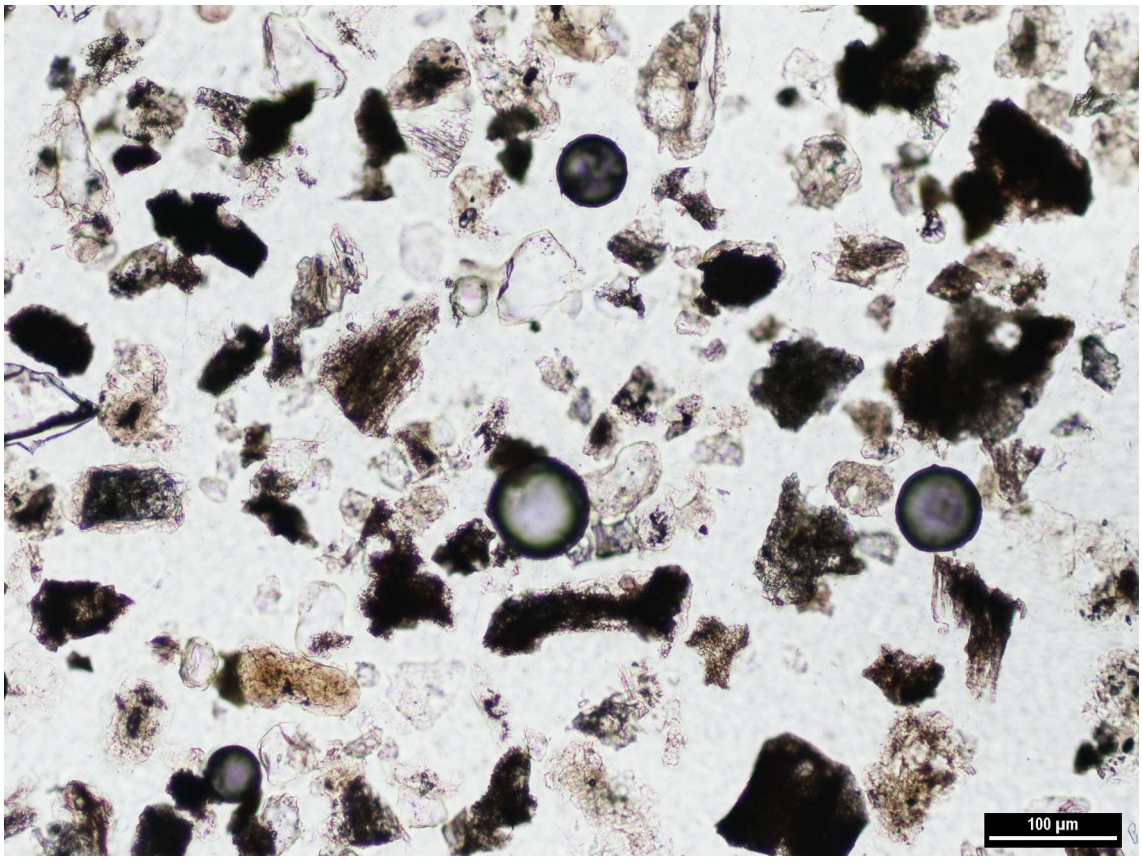

Figure 7. Optical microscope image of cryptotephra shards present in Keilambete samples, inclusions are visible as black fragments within glass. Note scale bar is 100 microns.

Due to the small separation in space observed when attempting to distinguish sites through a linear discriminant analysis, a KS-test was performed upon Mt Gambier and Mt Schank to determine if the difference observed between the two throughout the analysis was statistically significant. The results of the test show p-values below 0.05 for every major oxide analysed, indicating that each oxide is significantly different between the two sites at 95% confidence. However, it is possible that samples were taken from too few sites around Mt Gambier, and the full range of composition across the 14 eruption vents (van Otterloo et al., 2014) was not analysed, leading to a less accurate analysis.

Based upon these results, it is possible to distinguish the young volcanoes Mt Gambier and Mt Schank through the analysis of major oxide as a result of LA ICP-MS. However,

the LA ICP-MS analysis of microscopic cryptotephra shards results in significantly decreased accuracy in comparison to larger shards, such that Noorat and Warrnambool could not be successfully distinguished based upon their major oxides using LA ICP-MS. The electron microprobe analysis data, using the same statistical techniques has been shown to result in less scatter and smaller compositional ranges, resulting in more accurate differentiation between volcanoes. Subsequently, these results suggest that at the present LA ICP-MS may not be a precise enough tool to differentiate cryptotephra shards with sufficient accuracy for quantitative geochemical fingerprinting.

5.2. The usage of Trace element to discriminate volcanic glass providence

A variety of statistical tests have been carried out upon the trace element concentrations within Victorian cryptotephra and Mt's Gambier and Schank tephra to investigate its use as a discriminatory tool in geochemical analysis, with varied results.

The box plots of Mt Gambier and Schank data shows that the concentration of trace elements cluster well and contain few outliers for the majority of elements, with interquartile ranges that rarely exceeded a ± 20% difference from the median value, and differences greater than 1.35 standard deviations between the trace element concentrations of one another, indicating only small differences are present within concentrations across each of the two volcanoes. However, there was significantly greater difficulty in separating these trace elements concentrations from the other sites within the NVP. Due to the large interquartile ranges of the Victorian cryptotephra from sites Terang, Wangoom and Warrnambool, which often exceeded ± 100%, only a few elements; such as Y in the case of Mt Gambier, and Nb in Mt Schank could be differentiated from every other volcano tested based on their high concentrations. This suggests that the volcanoes either possess a large range of elemental compositions

across their eruption vents, or the samples possessed high uncertainty leading to inaccurate compositions as a result of their small size.

Linear discriminant analysis of the data could not isolate Warrnambool, Noorat or Eccles from other sites. However, it was able to find grouping for Terang, which the major oxide LDA was incapable of distinguishing from other sites, and suggests that these sites can be discriminated by their respective concentrations of Cs, Pr, Eu, Ta and Pb, which does not agree with the box plot diagrams.

The regression tree supported the results of the LDA, as the tree was capable of separating the same sites as the LDA analysis, such as Terang based upon Pb $\geq$ 0.00085%, U $\leq$ 0.00018% and Eu > 0.00011%, In addition, the regression tree was also capable of isolating Noorat though Pb $\leq$ 0.00085%, Rb < 0.0077%, Rb $\geq$ 0.004, Tm $\leq$ 2.6×10^{-5}, Eu > 0.0003 and Ce $\geq$ 0.011. However, only Eu and Pb coincide with the determined discriminatory elements found within the LDA, and, unlike the major oxide analysis, the trace regression tree was incapable of distinguishing Eccles.

The Trace element analysis, like the major oxide analysis was unable to isolate the geochemical fingerprint of Warrnambool. However, based upon its small sample size and large uncertainty values it is likely that it consisted of samples that were too small and few in number for an accurate analysis, rather than being too similar in composition to the other volcanic centres, and as a consequence, these data are inconclusive. Subsequently, these results suggest that volcanoes cannot be adequality distinguished based on singular marker elements (Sell and Samson, 2011), but rather their unique combination of trace elements. However, it is also possible that the large interquartile ranges associated with the Victorian cryptotephra samples may be due to error in the concentration resulting in the appearance of a wider range then actually exists.

Statistical analysis by means of a KS-test further supports this theory, as the p-values below 0.05 indicate that a statistically significant difference between Mt Gambier and Mt Schank, the 2 volcanoes analysed with little error, exists for all trace elements analysed except Dy and Tm.

The LA ICP-MS data obtained from Mt Gambier and Mt Schank possessed few samples with trace elements below the limit of detection, and uncertainty values that rarely exceeded 10% of the recorded concentration, suggesting that LA ICP-MS is capable of analysing the trace element concentration of large tephra grains with a relatively high degree of accuracy (Westgate et al., 1994). However, Unlike the data obtained at Mt's Gambier and Schank, the LA ICP-MS data gathered from the Victorian cryptotephra samples possessed many samples with elements below the detection limit which had to be removed from the analysis, and of those that were detectable, many possessed a high degree of uncertainty above 30% (Table 1). This further suggests that trace elemental analysis of cryptotephra shards is incapable of analysing tephra shards below 20 microns with a sufficient level of accuracy for accurate statistical analysis.

The statistical analysis of the data indicates that the small number of measurable samples, in addition to the amount of noise present within cryptotephra analysis results in the trace elements being of limited use in improving discrimination for samples below 20-microns in diameter. However, it is significantly more useful for improving discrimination in the case of large tephra shards such as those sampled at Mt's Gambier and Schank, which possess a wide concentration range for major oxides across its eruption vents due to their complexity, and can have difficulty distinguishing from other eruption centres based upon those oxides.

5.3 Improvements and future research

In the case of future research, all analysis should be performed using a non-siliceous mount during LA ICP-MS of volcanic tephra, such as epoxy resin (Pearce, 2014). This will result in a negligible increase in indicative elements should the laser ablate through the tephra into the mount, as the glass slides used in the samples obtained from Sarah Coulter contained elements that were analysed, which may have contributed to the large degree of uncertainty in those samples.

Future research into the effects of volcanoes possessing multiple eruptions vents should be explored. Sampling was taken from few sites within the Mt Gambier and Mt Schank eruption centres, but both volcanoes possess multiple eruption vents which can potentially possess small variations in geochemical composition. It is possible that if the full range of elements across each volcano was determined, it could result in a more precise geochemical fingerprint for each volcano. In addition, further sampling should be taken from the sites within Victoria. The cryptotephra samples used within the analysis were few in number, and often sizes below the recommended limit for LA ICP-MS, resulting in few samples being fit for analyses and large uncertainty values. Increased sampling from these sites would result in more tephra of a size amenable for accurate analysis. Alternatively, a 5-micron laser may be suitable for analysis of cryptotephra grains (Lowe et al., 2017) however this method also contains a number of drawbacks. 5-micron lasers are both more expensive to use, and are capable of analysing a smaller quantity of material, putting more pressure on the accuracy of the mass spectrometer (Pearce et al., 2011).

The statistical analysis techniques should be revised and adapted to incorporate uncertainty into the tests. Due to the small variations in geochemical concentration between volcanoes, the uncertainty associated with each element may be enough cause

the statistical analysis to give erroneous results. However, this means an alternate method of statistical analysis will need to be determined, as the program used in this analysis is not capable of incorporating uncertainty into the analysis. An alternate method of minimising uncertainty would also be to increase sampling so it is possible to remove samples with uncertainty above 2 standard deviations.

A further potential improvement for the analysis would be to do a full KS-Test for the statistical significance of every analysed element within each volcano prior to other statistical analysis. The removal of non-statistically significant elements would lead to a reduction in noise within the analysis and improved differentiation.

At the present, further research is required in order to test whether the method of LA ICP-MS is a viable technique towards the analysis of microscopic cryptotephra grains.

CONCLUSION

On the basis of the results of the conducted experiments, it appears that 8 of the 9 volcanic centres analysed within this experiment can be distinguished through LA ICP-MS based upon their trace and major elements with some accuracy. This was determined using a number of statistical analysis for isolating distinct geochemical concentration variations between sites, through the use of box plots, linear discrimination analysis and regression trees in conjunction to determine variation between sites in and locate key indicative elements for each site. Furthermore, it was determined that the addition of trace elements to a major oxide analysis will lead to improved discrimination in samples above 20 microns.

ACKNOWLEDGMENTS

I would like to thank my supervisors, Dr Jonathan Tyler and Dr Lee Arnold for their support and guidance throughout the year. I would also like to thank Dr Sarah Gilbert at

Adelaide Microscopy for her assistance in laboratory work to obtain and process LA analysis of volcanic samples. I would also like to thank Sarah Coulter for supplying volcanic samples for this project.

REFERENCES

ABBOTT, P., AUSTIN, W., DAVIES, S., PEARCE, N., AND HIBBERT, F. 2013. Cryptotephrochronology of the Eemian and the last interglacial-glacial transition in the North East Atlantic. *Journal Of Quaternary Science* 28, 501-514.

BARBETTI, M., AND SHEARD, M. 1981. Palaeomagnetic results from Mounts Gambier and Schank, South Australia. *Journal Of The Geological Society Of Australia* 28, 385-394.

BLACKBURN, G., ALLISON, GB., AND LEANEY, FWJ. 1982. Further evidence on the age of tuff at Mt Gambier, South Australia. Transactions of the Royal Society of South Australia, 106(3 & 4), 163-7

BLOCKLEY, S., PYNE-O'DONNELL, S., LOWE, J., MATTHEWS, I., STONE, A., POLLARD, A., TURNEY, C., AND MOLYNEUX, E. 2005. A new and less destructive laboratory procedure for the physical separation of distal glass tephra shards from sediments. *Quaternary Science Reviews* 24, 1952-1960.

BOYCE, J., KEAYS, R., NICHOLLS, I., AND HAYMAN, P. 2014. Eruption centres of the Hamilton area of the Newer Volcanics Province, Victoria, Australia: pinpointing volcanoes from a multifaceted approach to landform mapping. *Australian Journal Of Earth Sciences* 61, 735-754.

COULTER, S.E., 2007. The geochemical characterization and chronological significance of Quaternary tephra deposits in Greater Australia. Ph.D. thesis, Queen's University Belfast, UK

COULTER, S., TURNEY, C., KERSHAW, P., AND RULE, S. 2009. The characterization and significance of a MIS 5a distal tephra on mainland Australia. *Quaternary Science Reviews* 28, 1825-1830.

CURRAN, J. 2017. Hotelling: Hotelling's T^2 Test and Variants. (Auckland, NZ: CRAN).

DAVIES, S. 2015. Cryptotephras: the revolution in correlation and precision dating. *Journal Of Quaternary Science* 30, 114-130.

D'ANJOU, R., BALASCIO, N., AND BRADLEY, R. 2014. Locating cryptotephra in lake sediments using fluid imaging technology. *Journal Of Paleolimnology* 52, 257-264.

DEMIDJUK, Z., TURNER, S., SANDIFORD, M., GEORGE, R., FODEN, J., AND ETHERIDGE, M. 2007. U-series isotope and geodynamic constraints on mantle melting processes beneath the Newer Volcanic Province in South Australia. *Earth And Planetary Science Letters* 261, 517-533.

DUINTJER TEBBENS, J., AND SCHLESINGER, P. 2007. Improving implementation of linear discriminant analysis for the high dimension/small sample size problem. *Computational Statistics & Data Analysis* 52, 423-437.

GOURAMANIS, C., DE DECKKER, P., SWITZER, A., AND WILKINS, D. 2013. Cross-continent comparison of high-resolution Holocene climate records from southern Australia — Deciphering the impacts of far-field teleconnections. *Earth-Science Reviews* 121, 55-72.

HANSON, G. 1980. Rare Earth Elements in Petrogenetic Studies of Igneous Systems. *Annual Review Of Earth And Planetary Sciences* 8, 371-406.

HELLSTROM, J., PATON, C., WOODHEAD, J.D., AND HERGT, J. 2008. Iolite: software for spatially resolved LA-(quad and MC) ICPMS analysis. Mineralogical Association of Canada short course series. 40. 343–348.

HOUSLEY, R., MACLEOD, A., NALEPKA, D., JUROCHNIK, A., MASOJĆ, M., DAVIES, L., LINCOLN, P., BRONK RAMSEY, C., GAMBLE, C., AND LOWE, J. 2013. Tephrostratigraphy of a Lateglacial lake sediment sequence at Węgliny, southwest Poland. *Quaternary Science Reviews* 77, 4-18.

JORDAN, S., JOWITT, S., AND CAS, R. 2014. Origin of temporal - compositional variations during the eruption of Lake Purrumbete Maar, Newer Volcanics Province, southeastern Australia. *Bulletin Of Volcanology* 77,.

LEANEY, F., ALLISON, G., DIGHTON, J., AND TRUMBORE, S. 1995. The age and hydrological history of Blue Lake, South Australia. *Palaeogeography, Palaeoclimatology, Palaeoecology* 118, 111-130.

LOWE, D. 1992. Profile Descriptions of Quaternary Basaltic Volcanogenic Soils of the Mount Gambier Area, Southeast South Australia CSIRO Technical Report 9/1992, CSIRO division of soils, Adelaide, South Australia.

LOWE, D. 2011. Tephrochronology and its application: A review. *Quaternary Geochronology* 6, 107-153.

LOWE, D. J., AND ALLOWAY, B. V. 2015. Tephrochronology. In: RIN K, W. J., THOMPSON, J. W. (editors), Encyclopaedia of Scientific Dating Methods. Springer, Dordrecht, 733-799.

LOWE, D.J.; CHURCHMAN, G.J.; MERRY, R.H. ; FITZPATRICK, R.W., AND SHEARD, M.J.; HUDNALL, W.H. 1996. Holocene basaltic volcanogenic soils of the Mt Gambier area, South Australia, are unusual globally: what do they tell us? *Proceedings ASSSJ and NZ.SSS National Soils _Conference*, 1-4 July, University of Melbourne, 2, 153-154.

LOWE, D.J., AND PALMER, D.J. 2005. Andisols of New Zealand and Australia. Journal of Integrated Field Science, 2, 39-65.

LOWE, D., PEARCE, N., JORGENSEN, M., KUEHN, S., TRYON, C., AND HAYWARD, C. 2017. Correlating tephras and cryptotephras using glass compositional analyses and numerical and statistical methods: Review and evaluation. *Quaternary Science Reviews* 175, 1-44.

OKSANE, J., BLANCHE, F., FRIENDLY, M., KINDT, R., LEGENDR, P., MCGLINN, D., MINCHIN, P., O'HARA, R., SIMPSON, G., SOLYMOS, P., STEVENS. M.H.H., SZOECS, E., AND WAGNER, H. 2017. Vegan: Community Ecology Package R package version 2.4-4.

PEARCE, N. 2012. Laser ablation ICP-MS analysis of individual glass shards from tephra deposits – recent developments in trace element micro-analysis and Pb isotope determination. *Quaternary International* 279-280, 371.

PEARCE, N. 2014. Towards a protocol for the trace element analysis of glass from rhyolitic shards in tephra deposits by laser ablation ICP-MS. *Journal Of Quaternary Science* 29, 627-640.

PEARCE, N., DENTON, J., PERKINS, W., WESTGATE, J., AND ALLOWAY, B. 2007. Correlation and characterisation of individual glass shards from tephra deposits using trace element laser ablation ICP-MS analyses: current status and future potential. *Journal Of Quaternary Science* 22, 721-736.

PEARCE, N., PERKINS, W., WESTGATE, J., AND WADE, S. 2011. Trace-element microanalysis by LA-ICP-MS: The quest for comprehensive chemical characterisation of single, sub-10 μm volcanic glass shards. *Quaternary International* 246, 57-81.

PETRELLI, M., LAEGER, K., AND PERUGINI, D. 2016. High spatial resolution trace element determination of geological samples by laser ablation quadrupole plasma mass spectrometry: implications for glass analysis in volcanic products. *Geosciences Journal* 20, 851-863.

R CORE TEAM. 2013. R: A language and environment for statistical computing. R Foundation for Statistical Computing, Vienna, Austria.

Sell, B., and Samson, S. 2011. A tephrochronologic method based on apatite trace-element chemistry. *Quaternary Research* 76, 157-166.

SHERWOOD, J & OYSTON, B & KERSHAW, PETER. 2004. The age and contemporary environments of Tower Hill volcano, southwest Victoria, Australia. Proceedings of the Royal Society of Victoria. 116. 71-76.

SMITH, B., AND PRESCOTT, J. 1987. Thermoluminescence dating of the eruption at Mt Schank, South Australia. *Australian Journal Of Earth Sciences* 34, 335-342.

SMITH, R., TYLER, J., REEVES, J., BLOCKLEY, S., AND JACOBSEN, G. 2017. First Holocene cryptotephras in mainland Australia reported from sediments at Lake Keilambete, Victoria, Australia. *Quaternary Geochronology* 40, 82-91.

THERNEAU, T., ATKINSON, B., AND RIPLEY, B. 2017. rpart: Recursive Partitioning and Regression Trees. R package version 4.1-11.

VAN OTTERLOO, J., AND CAS, R. 2013. Reconstructing the eruption magnitude and energy budgets for the pre-historic eruption of the monogenetic ~5 ka Mt. Gambier Volcanic Complex, south-eastern Australia. *Bulletin Of Volcanology* 75,.

VAN OTTERLOO, J., CAS, R., AND SHEARD, M. 2013. Eruption processes and deposit characteristics at the monogenetic Mt. Gambier Volcanic Complex, SE Australia: implications for alternating magmatic and phreatomagmatic activity. *Bulletin Of Volcanology* 75,.

VAN OTTERLOO, J., RAVEGGI, M., CAS, R., AND MAAS, R. 2014. Polymagmatic Activity at the Monogenetic Mt Gambier Volcanic Complex in the Newer Volcanics Province, SE Australia: New Insights into the Occurrence of Intraplate Volcanic Activity in Australia. *Journal Of Petrology* 55, 1317-1351.

VENABLES, W. N. AND RIPLEY, B. D. 2002. Modern Applied Statistics with S. Fourth Edition. Springer, New York.

WESTGATE, J., PERKINS, W., FUGE, R., PEARCE, N., AND WINTLE, A. 1994. Trace-element analysis of volcanic glass shards by laser ablation inductively coupled plasma mass spectrometry: application to tephrochronological studies. *Applied Geochemistry* 9, 323-335.

APPENDIX A: MAJOR OXIDE ANALYSIS

LA ICP-MS Major oxides	Lambda values
Al2O3	548.1
Na2O	552.6
MgO	528.7
SiO	518.9
P2O5	546.2
K2O	513.7
CaO	521.4
TiO2	464.2
VO	3770
Cr2O3	393.5
MnO	505.6
FeO	523.9
SrO	-439.2
ZrO2	2341.6
BaO	303.1

Major oxide lambda values as derived from LDA

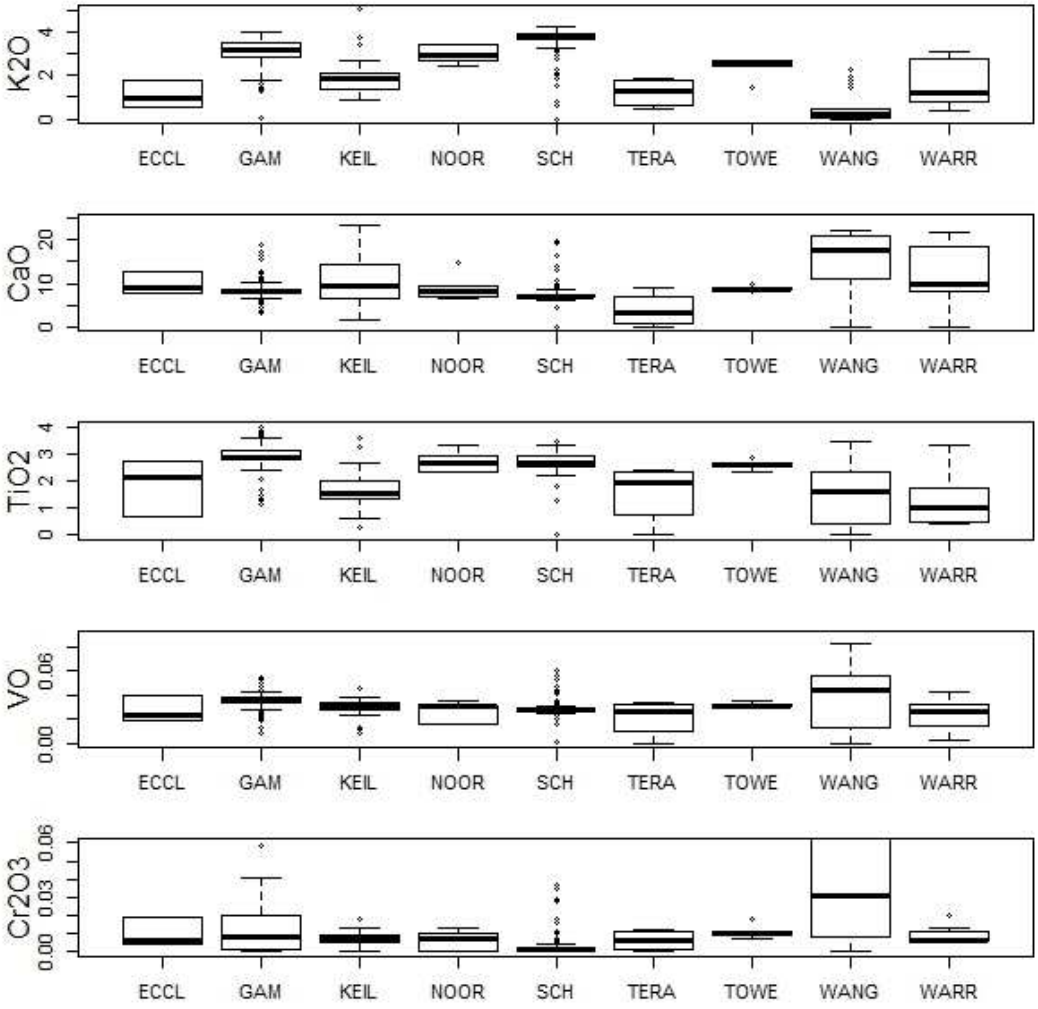
K2O
0
2
4
CaO
0
10
20
TiO2
0
1
2
3
4
VO
0.00
0.06
Cr2O3
0.00
0.03
0.06
ECCL
GAM
KEIL
NOOR
SCH
TERA
TOWE
WANG
WARR

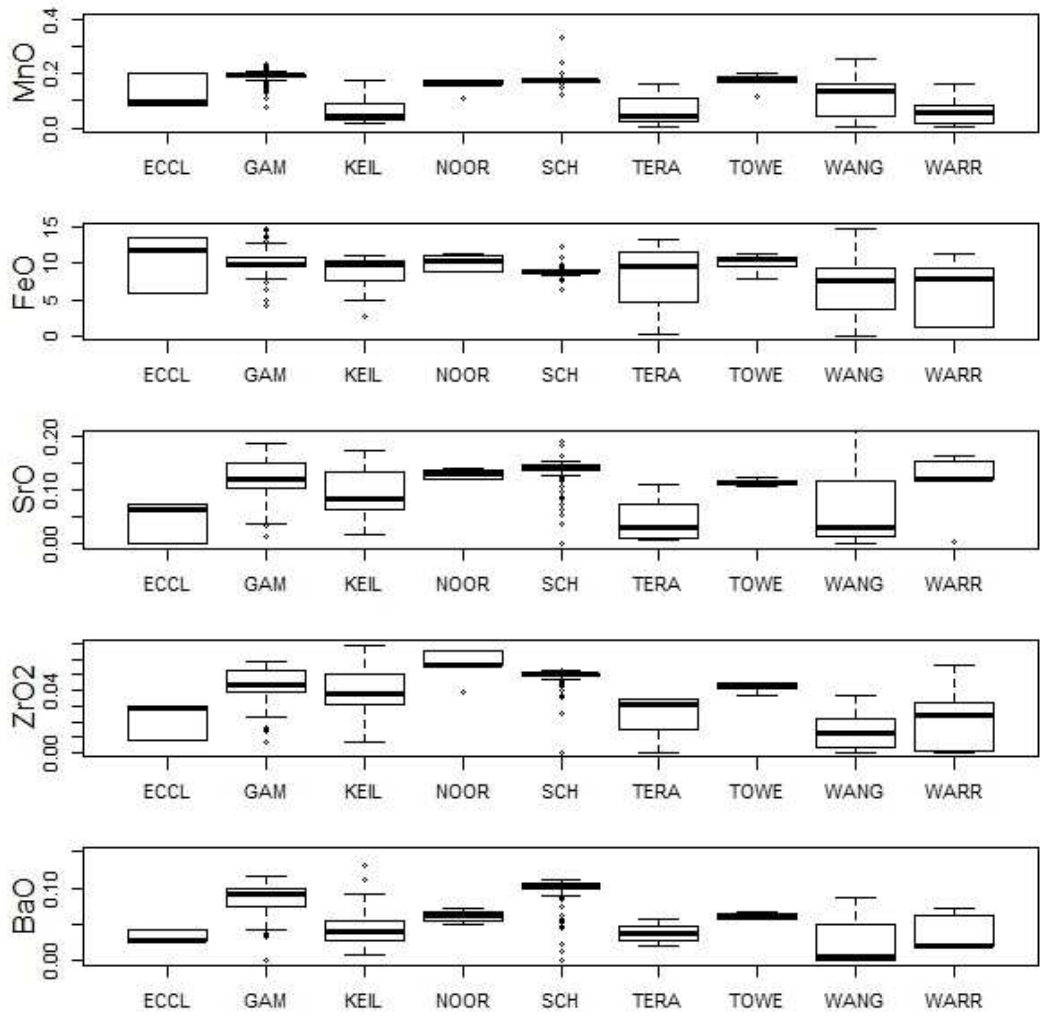

Major oxide box plot of oxides against each volcano, central black line is median, box represent interquartile range, dots represent outliers.

APPENDIX B: SARAH COULTER DATA AND ANALYSIS

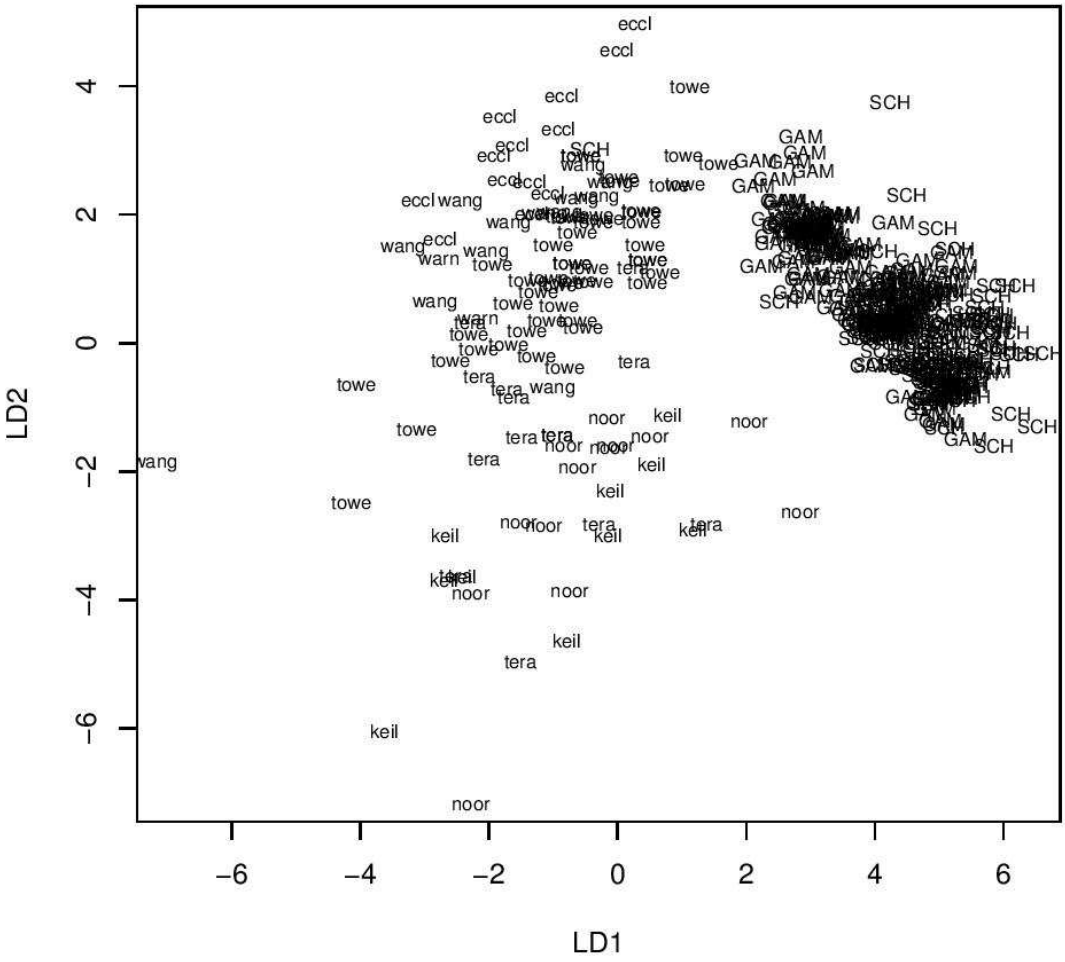

EM Major oxide	Lambda
Na2O	1.443
MgO	100.4
SiO2	-3.5
Al2O3	20.1
P2O5	-185.5
K2O	-141.8
CaO	56.5
TiO2	-299.8
MnO	-204.633
FeO	13.7

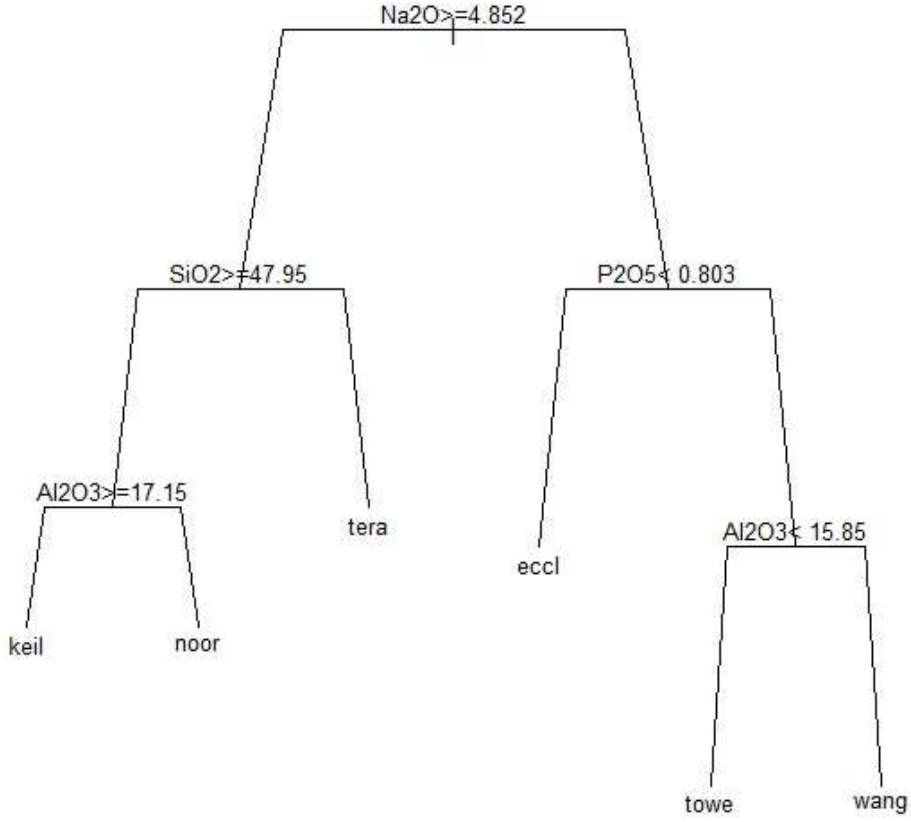
Na2O>=4.852
SiO2>=47.95
P2O5< 0.803
Al2O3>=17.15
tera
eccl
Al2O3< 15.85
keil
noor
towe
wang

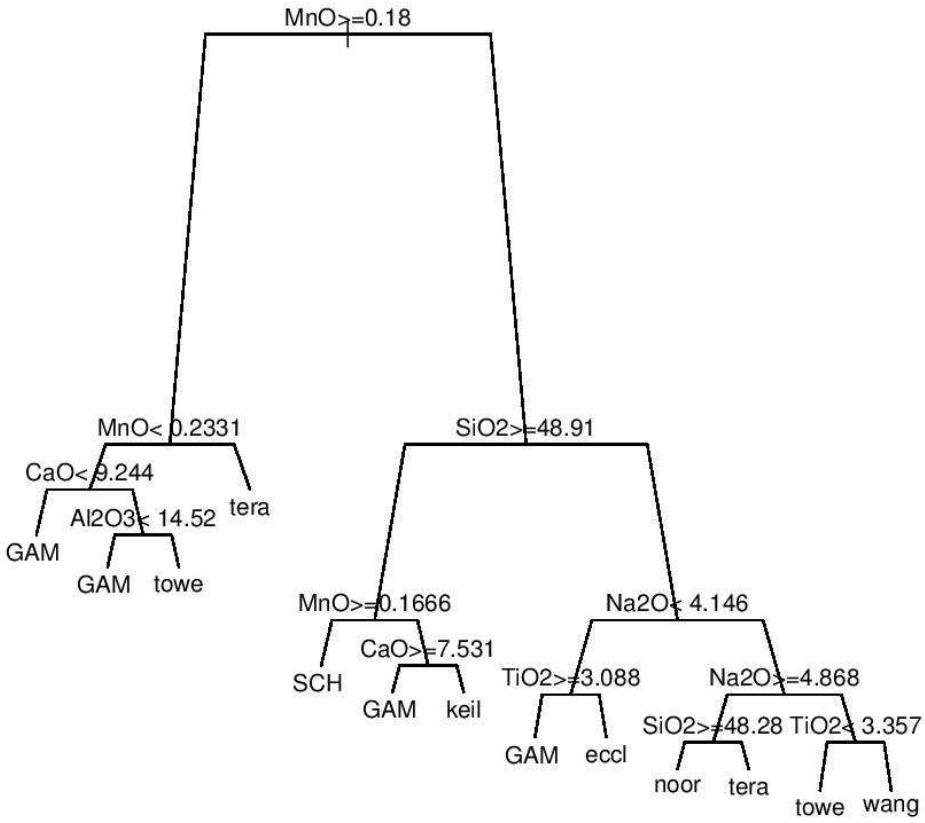
MnO>=0.18
MnO< 0.2331
SiO2>=48.91
CaO< 9.244
tera
Al2O3< 14.52
GAM
GAM
towe
MnO>=0.1666
Na2O< 4.146
CaO>=7.531
SCH
TiO2>=3.088
Na2O>=4.868
GAM
keil
GAM
eccl
SiO2>=48.28
TiO2< 3.357
noor
tera
towe
wang

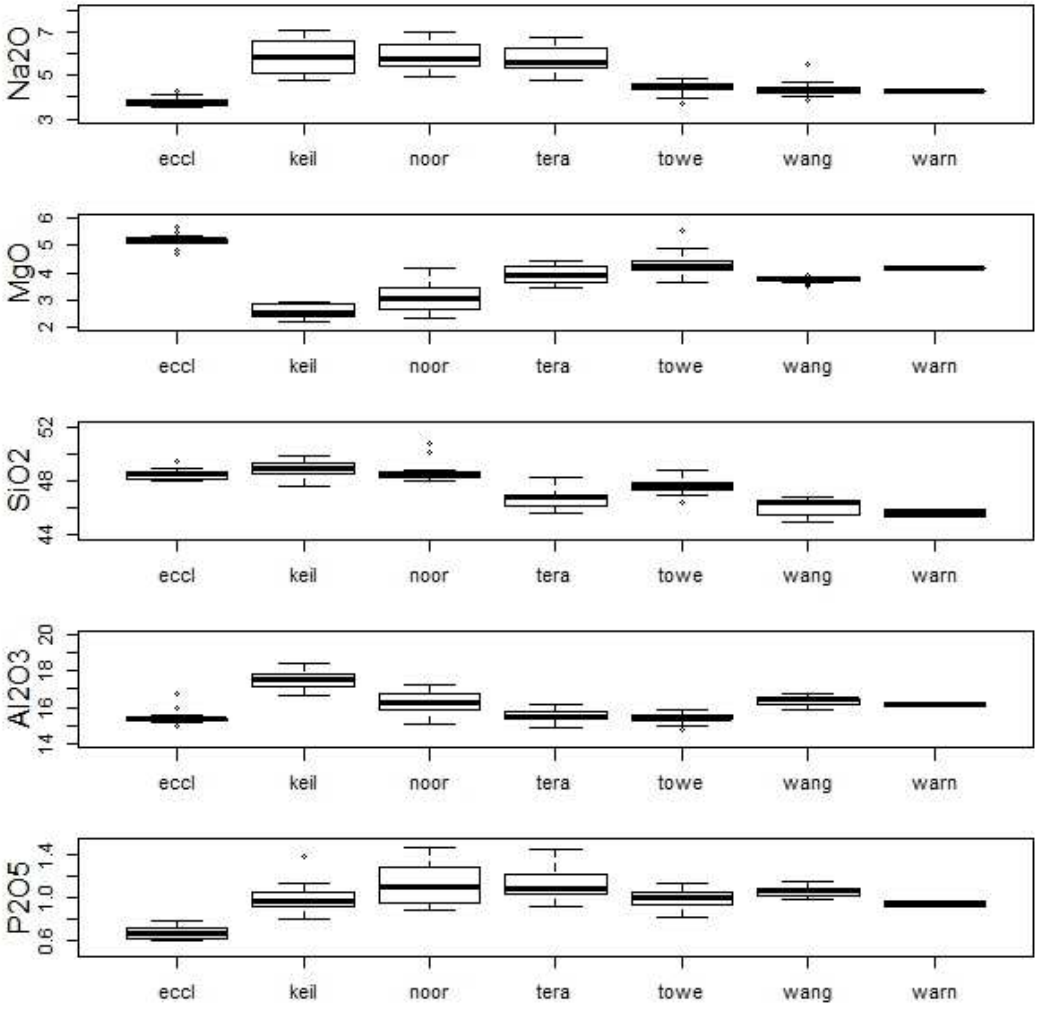
Na2O
3
5
7
MgO
2
3
4
5
6
SiO2
44
48
52
Al2O3
14
16
18
20
P2O5
0.6
1.0
1.4
eccl
keil
noor
tera
towe
wang
warn

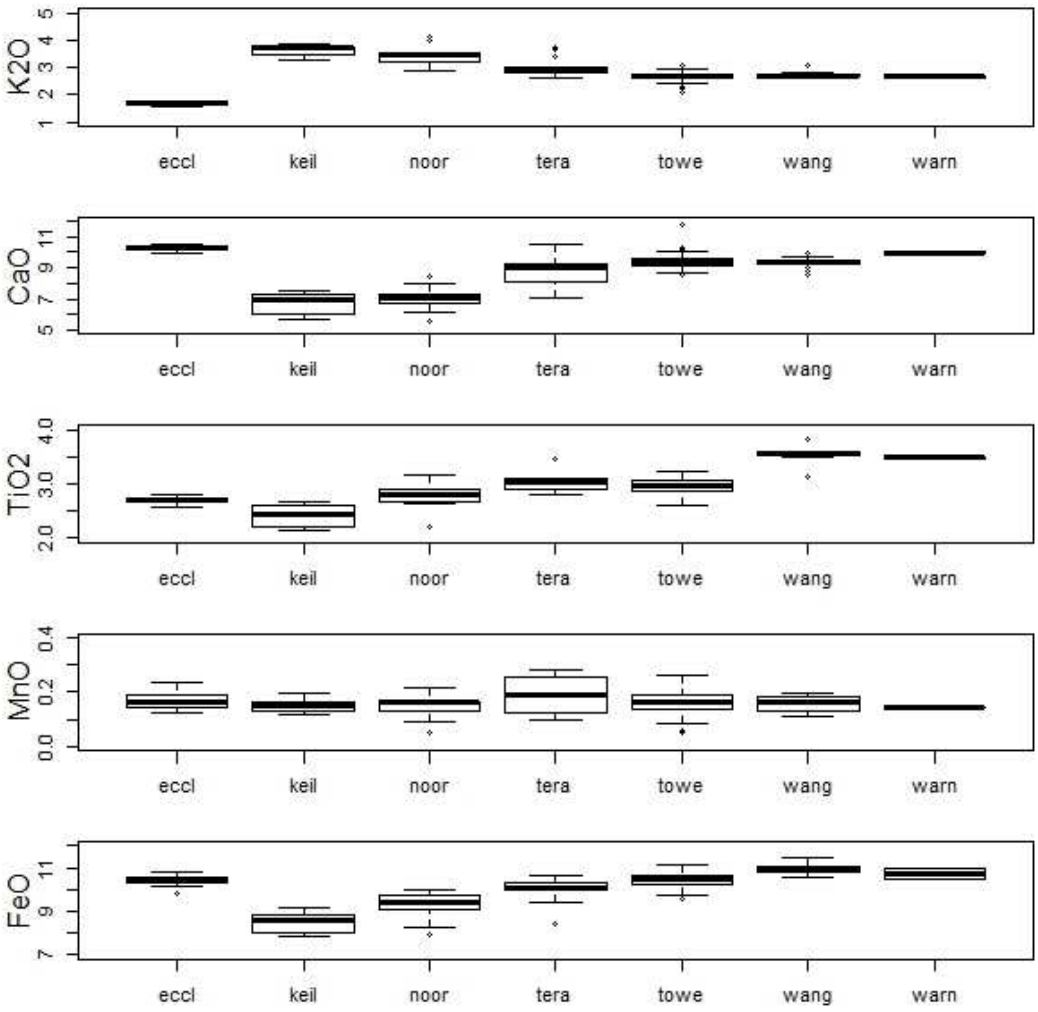
K2O
1 2 3 4 5
CaO
5 7 9 11
TiO2
2.0 3.0 4.0
MnO
0.0 0.2 0.4
FeO
7 9 11
eccl keil noor tera towe wang warn

APPENDIX C: TRACE ELEMENT ANALYSIS

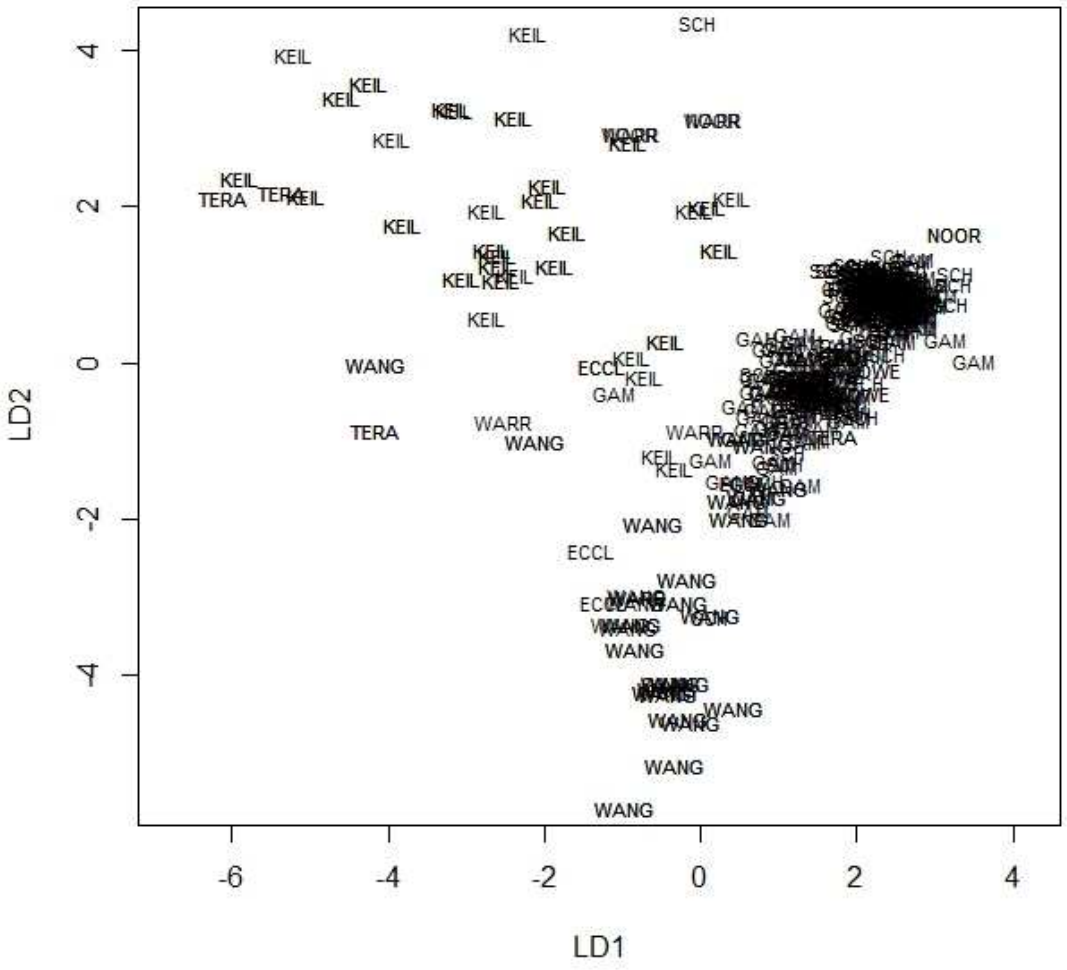

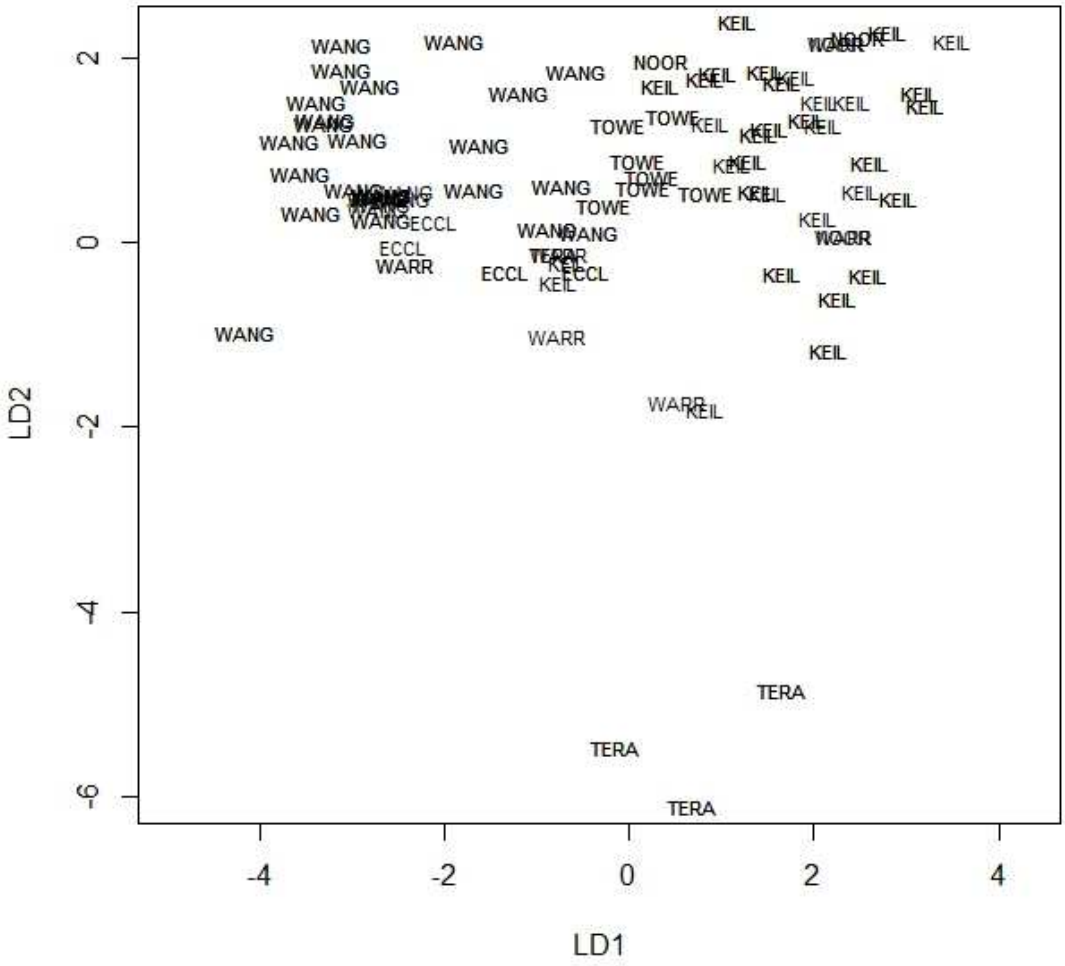

Trace Element	Lambda
Sc	-1532
Rb	-16436
Y	18229
Nb	12315
Cs	83410
La	-4977
Ce	-8752
Pr	72558
Nd	-9482
Sm	-13321
Eu	81339
Gd	6258
Dy	-1113
Hf	-48130
Ta	69571
Pb	67006
Th	-52713

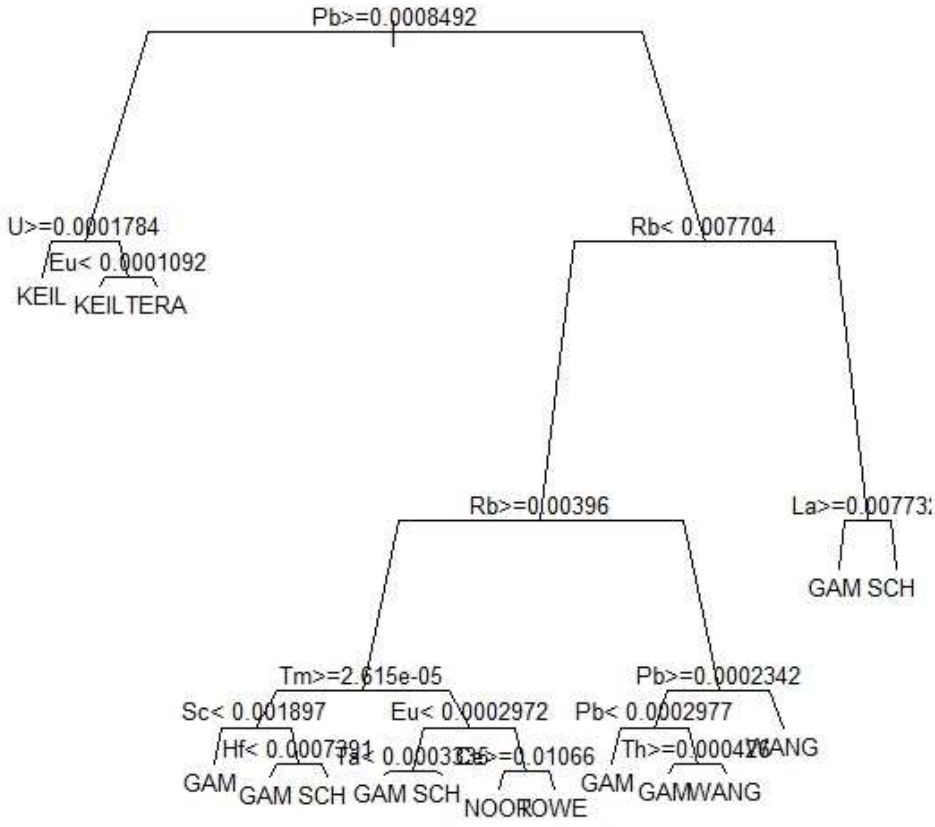
Pb>=0.0008492
U>=0.0001784
Eu< 0.0001092
KEIL
KEILTERA
Rb< 0.007704
Rb>=0.00396
La>=0.00773
GAM SCH
Tm>=2.615e-05
Pb>=0.0002342
Sc< 0.001897
Eu< 0.0002972
Pb< 0.0002977
Hf< 0.0007391
Ta< 0.0003126
Ce>=0.01066
Th>=0.0004276
ANG
GAM
GAM SCH
GAM SCH
NOOR
OWE
GAM
GAMWANG

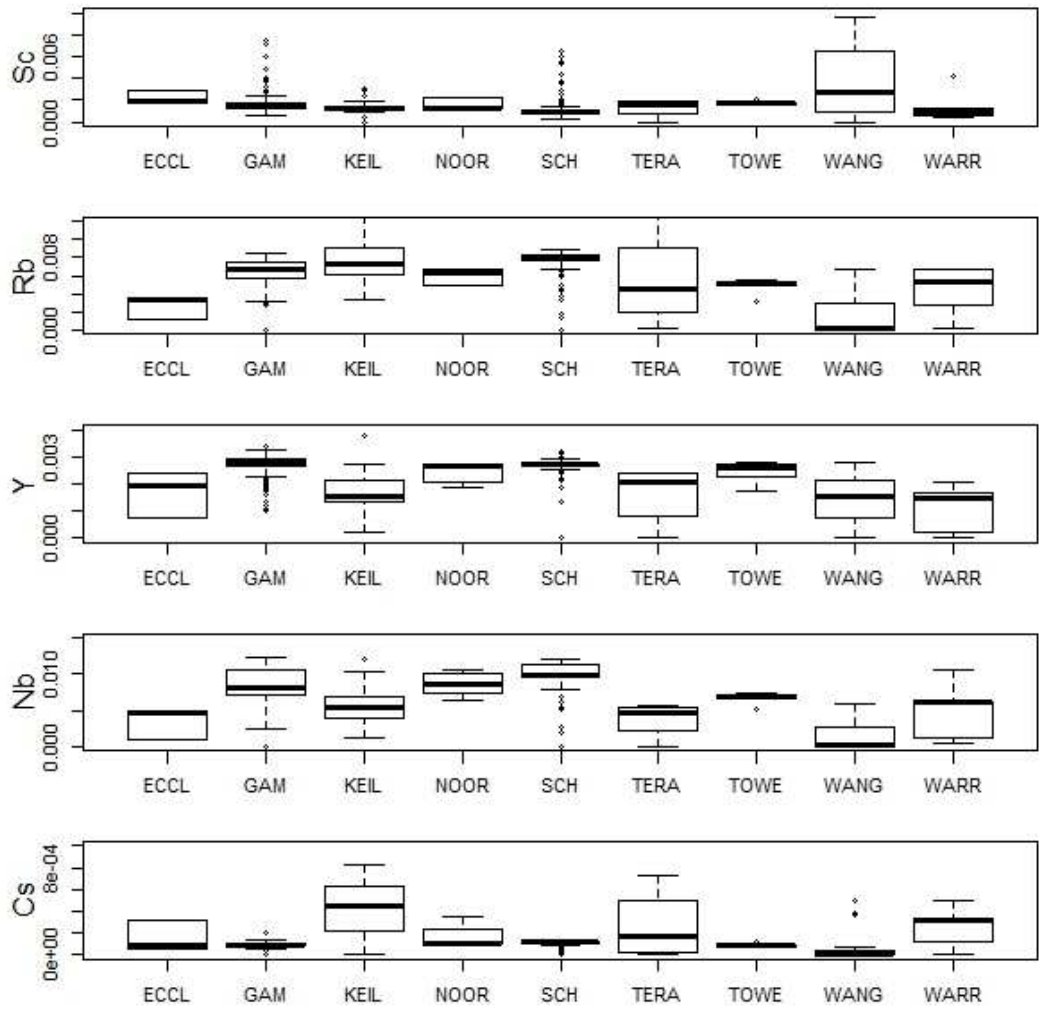
Sc
0.000
0.006
Rb
0.000
0.008
Y
0.000
0.003
Nb
0.000
0.010
Cs
0e+00
8e-04
ECCL
GAM
KEIL
NOOR
SCH
TERA
TOWE
WANG
WARR

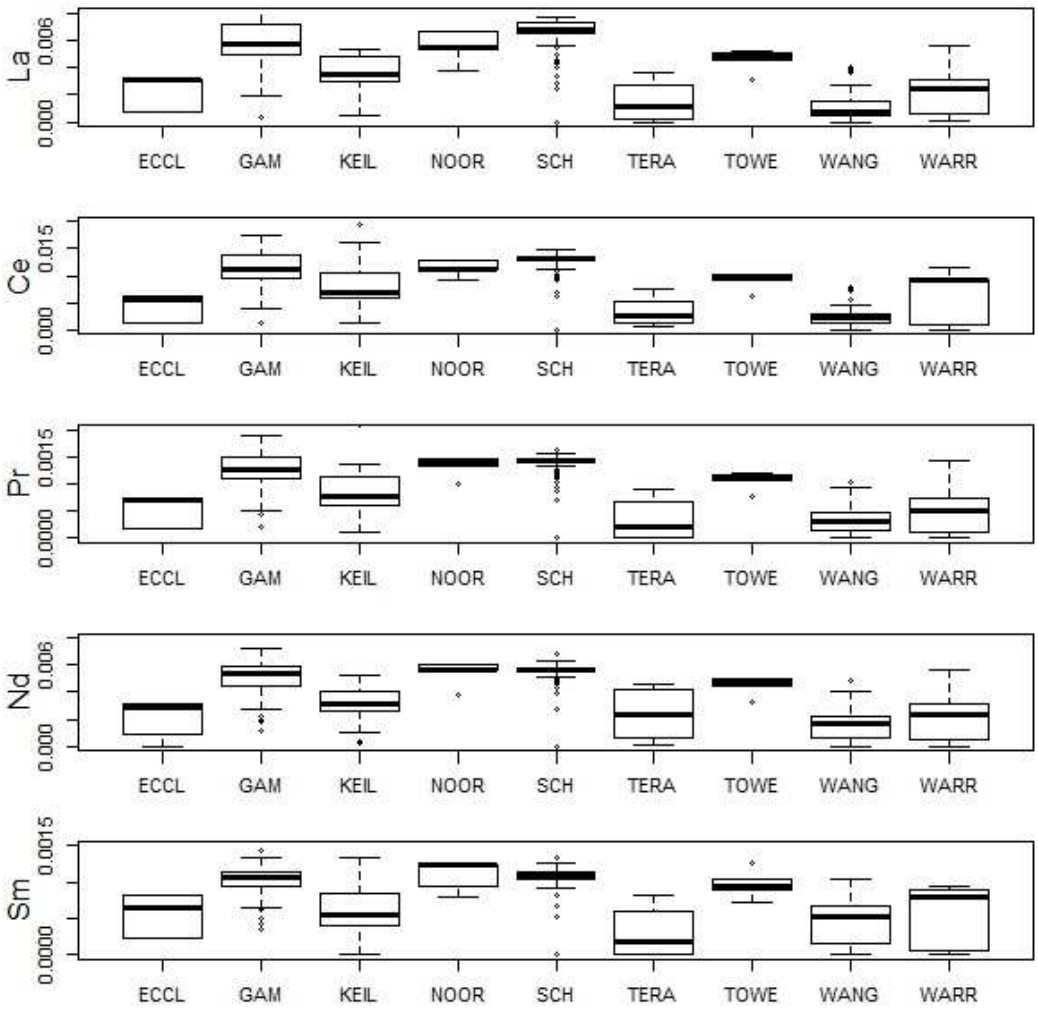
La
0.000
0.006
Ce
0.000
0.015
Pr
0.0000
0.0015
Nd
0.000
0.006
Sm
0.0000
0.0015
ECCL
GAM
KEIL
NOOR
SCH
TERA
TOWE
WANG
WARR

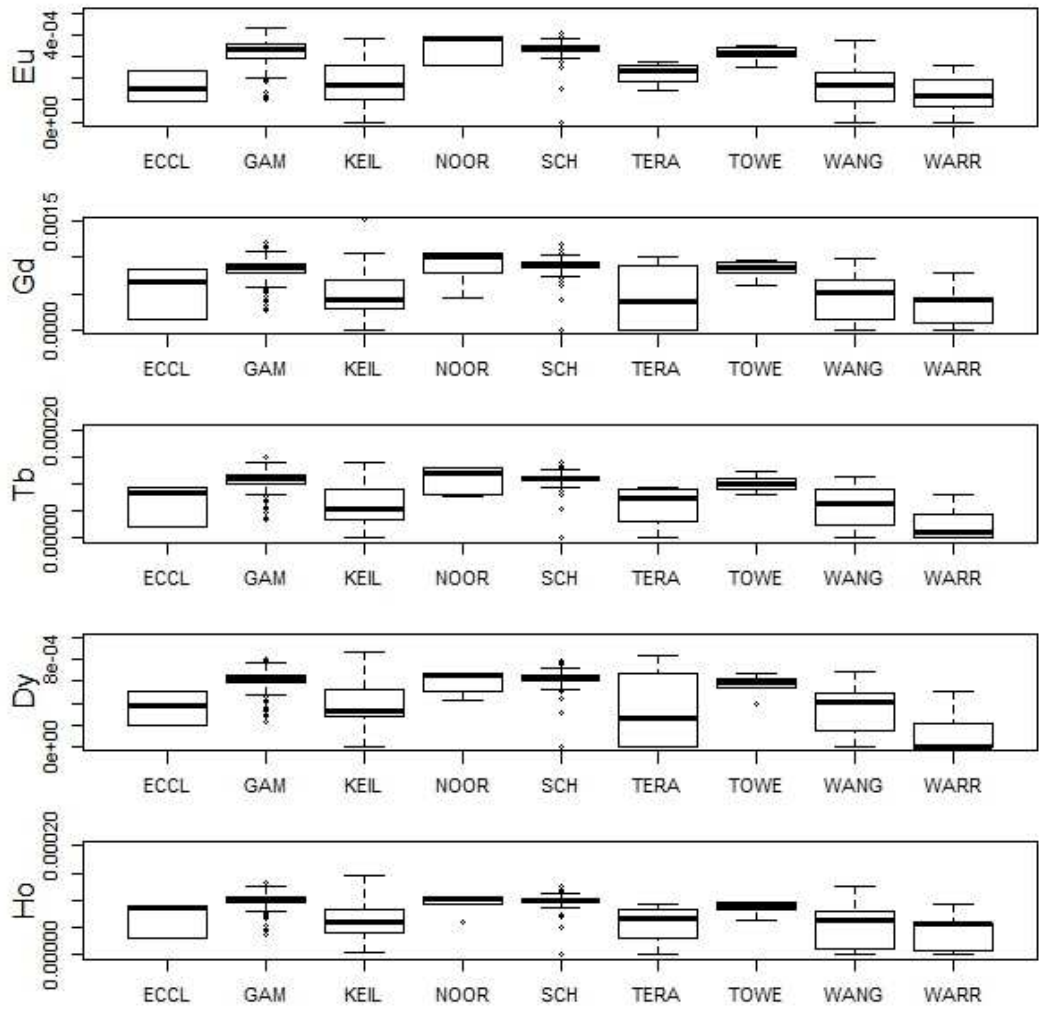
Eu
0e+00
4e-04
Gd
0.0000
0.0015
Tb
0.00000
0.00020
Dy
0e+00
8e-04
Ho
0.00000
0.00020
ECCL
GAM
KEIL
NOOR
SCH
TERA
TOWE
WANG
WARR

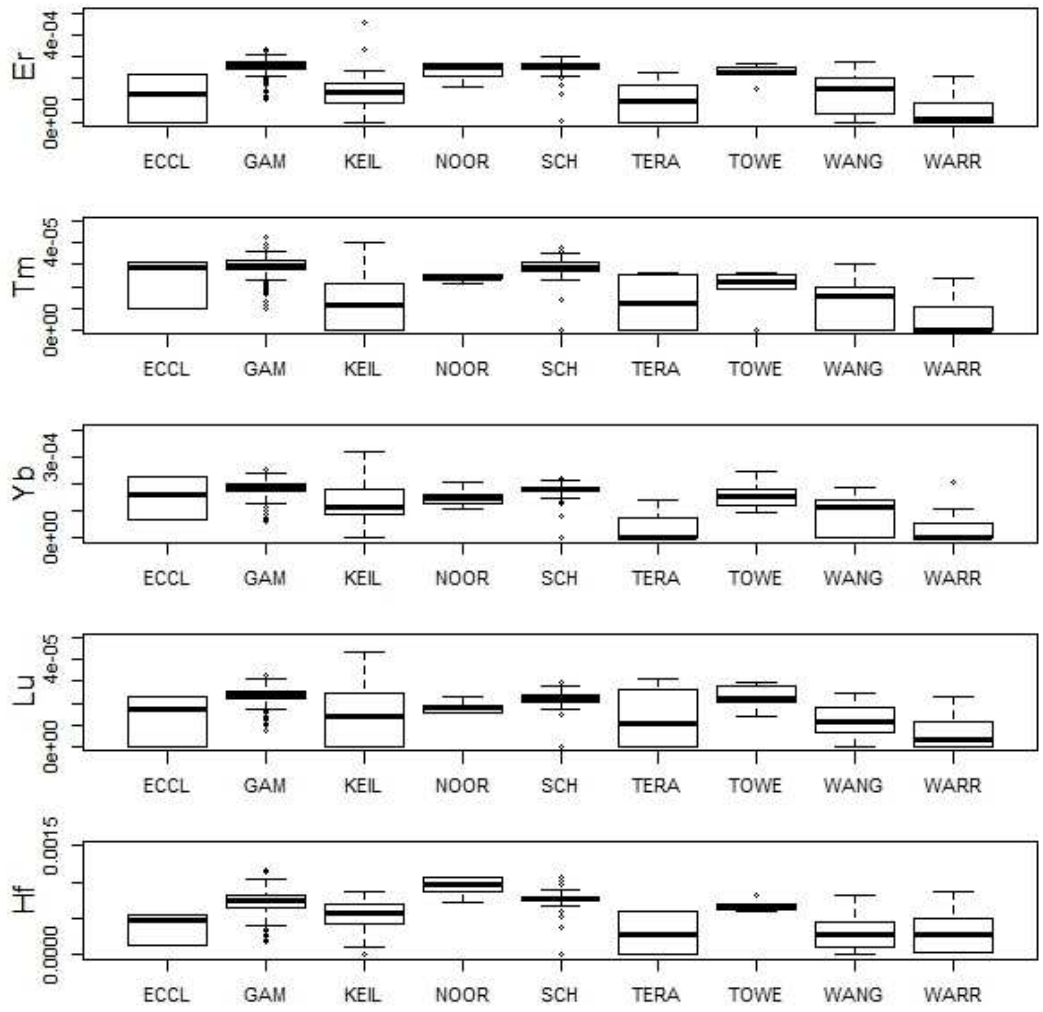
Er
0e+00
4e-04
Tm
0e+00
4e-05
Yb
0e+00
3e-04
Lu
0e+00
4e-05
Hf
0.0000
0.0015
ECCL
GAM
KEIL
NOOR
SCH
TERA
TOWE
WANG
WARR

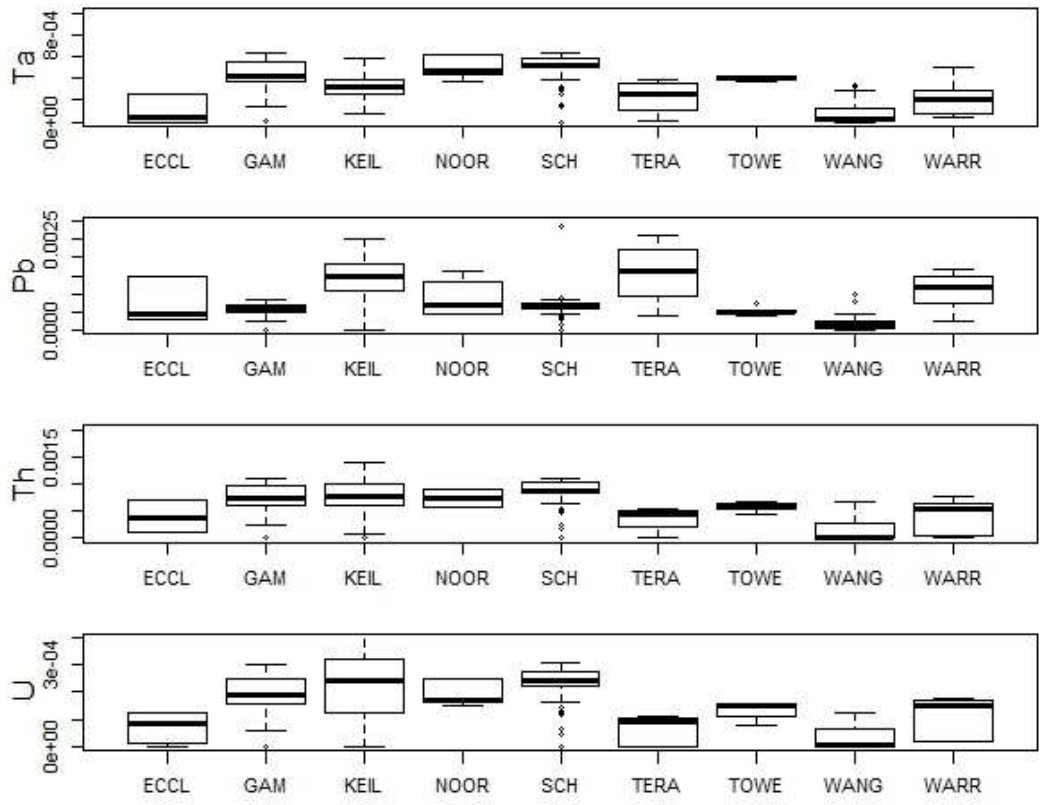
Ta
0e+00
8e-04
Pb
0.0000
0.0025
Th
0.0000
0.0015
U
0e+00
3e-04
ECCL
GAM
KEIL
NOOR
SCH
TERA
TOWE
WANG
WARR